Finite time blow-up of a singular parabolic problem

Beek, L.C. van

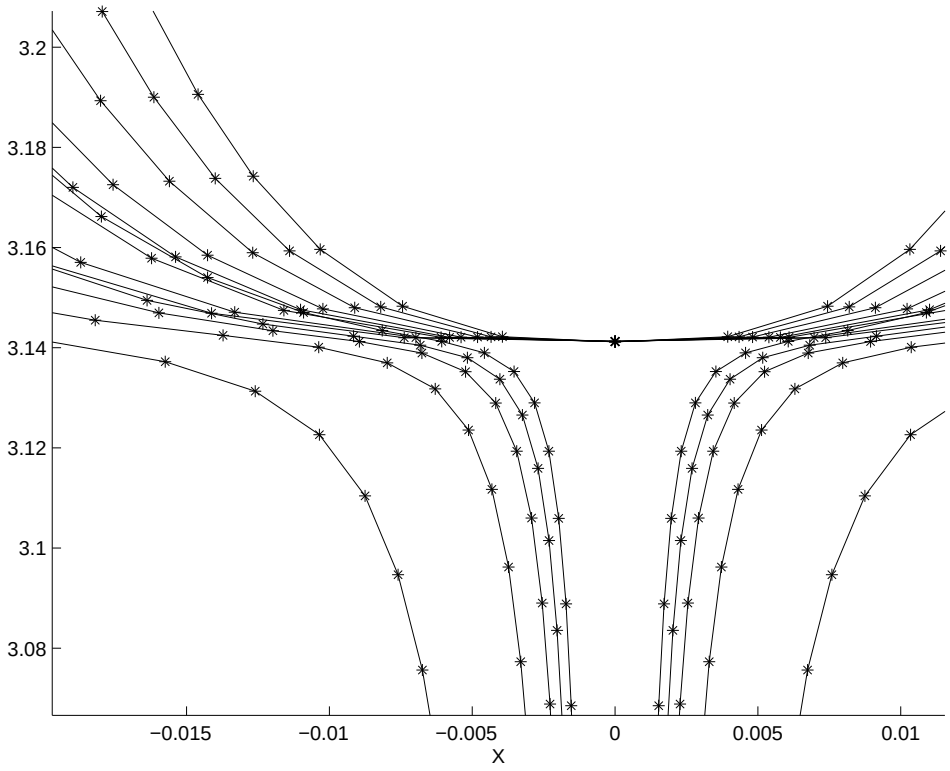

Finite time blow-up of a singular parabolic problem

Master Thesis of L. C. van Beek
Department of Mathematics, Leiden University
Supervisor: Prof. Dr. R. van der Hout

July 6, 2004

Contents

Preface

This report was written as a part of my graduation research project, which took place between fall 2001 and summer 2004. I would like to thank the following people for their support and cooperation:
First of all, Prof. Dr. R. van der Hout, who was my supervisor. I have learned a lot from our cooperation. I want to mention that I appreciated his enthousiasm for the subject matter and his patience in answering my questions.
Secondly, I want to thank Dr. P. Zegeling, who was kind enough to give me his moving grid code, which played a large role in my project. Without his code, it would have been much harder to obtain interesting numerical results for the problem that we studied.
Further thanks go out to Dr. F. Dekkers, with whom Prof. Van der Hout and I had a couple of stimulating discussions about the matters that are discussed in chapter 4 of this report.

There are many other people in the Mathematical Institute of Leiden University, and also beyond its borders, that supported me during this project. I thank them also for their help and cooperation. Hopefully, I do not forget to mention any substantial contributions at this point.
And last - but not least - I wish to thank my parents for their financial and moral support during the whole period of my studies.

Leiden, July 6, 2004,
Lucien van Beek

1 Introduction

This report is concerned with the blow-up behaviour of the harmonic map heat flow between surfaces. The problems studied here are special cases: we consider only the harmonic map heat flow corresponding to radially symmetric maps from the unit disk D^2 into the unit sphere S^2.

In this chapter, we shall first present the problems that were studied. In the second section, we will summarize the contents of this paper.

1.1 The problem

The harmonic map heat flow $u : \bar{D}^2 \times [0,T) \to S^2$, corresponding to an initial mapping $\phi : \bar{D}^2 \to S^2$, is described by the following system:

$$\begin{aligned} \frac{\partial u}{\partial t} &= \Delta u + |\nabla u|^2 u, && (1)\\ u(x,0) &= \phi(x), && (2)\\ u(\cdot,t)|_{\partial D^2} &= \phi|_{\partial D^2}. && (3) \end{aligned}$$

Here, $|\nabla u|^2 = \sum_{i,j} \left(\frac{\partial u_i}{\partial x_j}\right)^2$, by definition. Let $\phi : \bar{D}^2 \to S^2$ be radially symmetric. This means that it has the form

$$\phi(x) = \left(\frac{x}{|x|}\sin\psi(|x|), \cos\psi(|x|)\right), \qquad (4)$$

where $x \in D^2$ and $\psi : [0,1] \to \mathbb{R}$. As is shown in [3], the fact that the initial condition ϕ is radially symmetric implies that the solution u to (1)-(3), if it exists up to $t = T$, will be radially symmetric for all $t < T$ as well. So u can be written as

$$u(x,t) = \left(\frac{x}{|x|}\sin\theta(|x|,t), \cos\theta(|x|,t)\right), \qquad (5)$$

for some $\theta : [0,1] \times [0,T) \to \mathbb{R}$.

Let us consider D^2 and S^2 as embedded in $\mathbb{R}^3$. We equip $\mathbb{R}^3$ with cartesian coordinates $y = (y_1, y_2, y_3)$. Then let $D^2 = \{y_1^2 + y_2^2 \leq 1;\ y_3 = 0\}$ be a subset of the y_1y_2-plane, and let S^2 be the set $\{y_1^2 + y_2^2 + y_3^2 = 1\}$. Assume also that u maps the origin of D^2 to the north pole $N = (0,0,1)$ of the sphere[1].

$u \in S^2$ can be expressed in terms of the spherical coordinates: $y_1 = r\cos\varphi\sin\theta$, $y_2 = r\sin\varphi\sin\theta$ and $y_3 = r\cos\theta$. So $x = (r\sin\varphi, r\cos\varphi)$ for $x \in D^2$, and θ is the angle of u with the positive y_3-axis. From a straightforward calculation it follows then that the function $\theta(r,t)$ in (5) satisfies the parabolic problem[2]:

[1] Remark: this implies, by what follows, that $\theta(0,t) = k\pi$, which is an additional condition on θ that does not follow directly from problem (1)-(3). We shall justify this assumption in the next chapter.

[2] Unlike the initial condition and the boundary condition for $r = 1$, the boundary condition at $r = 0$ does not follow from the formulation in (3), but is imposed on the problem by energy considerations, to which we shall come back in section 2.3.

$$\theta_t = \theta_{rr} + \frac{1}{r}\theta_r - \frac{\sin 2\theta}{2r^2}, \tag{6}$$
$$\theta(r,0) = \psi(r), \tag{7}$$
$$\theta(0,t) = k\pi, \tag{8}$$
$$\theta(1,t) = \psi(1) := \Theta. \tag{9}$$

As usual, subscripts denote partial differentiation. The initial condition ψ is induced by (2) and (4). Without loss of generality, we shall assume in what follows - unless indicated otherwise - that $k = 0$.

In this paper we shall study the behaviour of the following, more general form of problem (6)-(9):

$$\theta_t = \theta_{rr} + \frac{1}{r}\theta_r - \frac{n^2 \sin 2\theta}{2r^2}, \tag{10}$$
$$\theta(r,0) = \psi(r), \tag{11}$$
$$\theta(0,t) = 0, \tag{12}$$
$$\theta(1,t) = \psi(1) := \Theta. \tag{13}$$

The motivation for the inclusion of the parameter n and for the relation between equations (6) and (10) will be given in chapter 2.

For $n = 1$, equation (10) reduces to (6), for which the behavior has been studied in [4] and [3]. A typical result for the situation $n = 1$ is the following: in the case $|\psi(1)| > \pi$, the solution $\theta(r,t)$ blows up in finite time, while in the case $|\psi(r)| \leq \pi \ \forall r \in [0,1]$, the solution $\theta(r,t)$ exists for all time. In any case, as $t \to \infty$, the solution will tend to a harmonic map[3], which is by definition an equilibrium solution of equation (1). Finite time blow-up means, when it occurs in this setting, that the solution $\theta(r,t)$ makes a jump over a multiple of π in $r = 0$.

Motivated by the results in [3] and [4], the main question that we tried to answer in our research is:

Question 1.1 (Main Question)*: For which values of the parameter n and under what conditions does the solution $\theta(r,t)$ to (10)-(13) blow up in finite time?*

It was expected that some N could be found (maybe even $N = 1$), such that finite time blow up would not occur when $n > N$.

[3]By abuse of the definition, we call here an equilibrium solution to (6), corresponding to (1) via (5), harmonic as well.

1.2 Contents of this paper

The plan was to tackle Question 1.1 by analytic means first. If those attempts would fail, we would try to find a suitable numerical scheme and say something about the occurence of blow-up in this numerical scheme. It turned out after some time that analytical tools had been developped by Van der Hout, Vilucchi and Bertsch (see [2]). These tools were sufficient to answer Question 1.1 for $n \neq 2$. For $n = 2$ results using formal asymptotics by Van den Berg, Hulshof and King became known which imply the global existence of a smooth solution, but there is no rigorous proof yet for this case. A small survey of these results will be given below in chapter 2.

Chapter 2 starts with a description of the physical and mathematical background of the problem; subsequently, some other results in this area will be discussed as well, such as those by Chang, Ding and Ye [4] and Van der Hout [7]. These are articles that I studied and used intensively during my project.

Because an analytical answer to Question 1.1 for $n = 2$ turned out to be hard to find, attention was turned to the numerical side of the problem. Chapter 3 contains my own attempts to find a suitable scheme approximating equation (10). However, these attempts were not successful. A new direction for my research was opened when I found some references to Dr. Paul Zegeling from Utrecht University. His algorithm for solving certain types of PDE using so-called moving grid methods turned out to be applicable to the current problem; moreover, it turned out that Dr. Fieke Dekkers (also from Utrecht) was working with Zegeling on this and related problems as well. My new project was to apply the Zegeling scheme to problem (10)-(13), to justify this application and to interpret deviations in the output from what was expected on basis of the analytical results.

In chapter 3 we will also describe the basic outlines of the moving grid method used in the Zegeling scheme. Moreover, we will discuss what results about blow-up phenomena we can expect to gain from a numerical approximation.

An attempt to justify the application of the Zegeling scheme will be discussed in chapter 4 below. There are two obstacles: first, the numerical scheme solves the equation on another domain (this obstacle can be removed easily). The other obstacle lies in the way of dealing with the singularity in $r = 0$. We will see that, if one discretizes time only, the blow-up behaviour of these semi-discrete solution is different from that of the analytical solutions.

The discussion of the output and explanations of the anomalies in the approximations will be the subject of chapter 5. Several suggestions are made about how to interpret the numerical approximations.

Finally, we will conclude by summarizing the (mainly numerical and interpretative) results and give some suggestions for future research on these problems.

2 Blow-up of the harmonic map heat flow: an overview

In this chapter, we will discuss the derivation of the equations and problems mentioned in the Introduction. We will also summarize some results on finite time blow-up that were obtained so far in this domain of research.

2.1 Some remarks about the physical setting

A way to motivate the study of the problems mentioned in the Introduction is to consider the physical model that has led to these equations. Problem (1)-(3) was derived in the study of Nematic Liquid Crystals (NLCs). A NLC is a kind of fluid consisting of long chain molecules. In [7] a situation is studied where the NLC is contained in a cylindrical tube, and is assumed to be incompressible. If we denote the local chain direction by u, physical arguments imply that a NLC, contained in a section Ω of the tube with unit length, has an energy given by

$$\mathcal{E}(u) = \frac{K}{2} \int_\Omega |\nabla u|^2 \, \mathrm{d}x, \tag{14}$$

where $|\nabla u|^2 = \sum_{i,j} \left(\frac{\partial u_i}{\partial x_j} \right)^2$ by definition, and K is a physical constant. By symmetry we may restrict our attention to a two-dimensional cross-section Ω perpendicular to the cylinder axis. So $\Omega = D^2$.

The energy we spoke of is some kind of elastic energy; it will be minimized if the molecules are parallel. $|\nabla u|^2$ measures the extent to which the molucules are "in line". The assumption made here is, that the alignment of the molecules, which determines the energy density, depends only on these partial derivatives. The Dirichlet conditions at the boundary of the tube determine that the direction field is radially symmetric around $r = 0$, provided the initial conditions are radially symmetric.

2.2 Remarks on the mathematical background of the problems

The general setting of the problem (1)-(3) studied here is that of harmonic mappings between Riemannian surfaces. Struwe [9] gives an overview of this domain of research. Harmonic maps u between surfaces M and M' are given by

$$\mathcal{L}u = 0, \tag{15}$$

where $\mathcal{L}$ is the Laplace-Beltrami operator (see any standard textbook on differential geometry for its definition). The harmonic map heat flow is then given by the equation

$$u_t = \mathcal{L}u$$

for $u : M \times (0,T) \to M'$, supplied with appropriate initial-boundary conditions. Problem (1)-(3) is a special case; in the following lines we sketch an intuitive way to look at this problem.

Why is a stationary solution to (1)-(3) called harmonic? For a function $v : \mathbb{R}^N \to \mathbb{R}^M$, the demand that $\Delta v = 0$ on a domain Ω is equivalent to

$$\int_\Omega |\nabla v|^2 \, \mathrm{d}x \text{ is minimal for } v \in \mathcal{F}$$

for a set of functions $\mathcal{F}$ for which this integral exists.

Consider now a set of mappings $\mathcal{F} \subset \{u : D^2 \to S^2\}$ such that for $u \in \mathcal{F}$, the following integral exists:

$$\int_\Omega |\nabla u|^2 \, \mathrm{d}x.$$

A minimizer of this integral over $\mathcal{F}$ is called harmonic. This is exactly the minimization problem that is derived from physical considerations in (14). The demand that $u \in \mathcal{F}$ implies that $||u|| = 1$. In physical terms, this means that we only consider normalized chain-direction vectors u.

To obtain a differential equation for the minimizer of the integral $\int_{D^2} |\nabla u|^2 \, \mathrm{d}x$, we apply a standard variational technique for constrained minimization. To be precise, given a candidate-minimizer u, we perturb $u(x)$ by a perturbation $\epsilon\,\xi(x) \in \mathbb{R}^3$, vanishing at ∂D^2 and such that $\langle u(x), \xi(x)\rangle = 0$ for all $x \in D^2$. The latter condition is needed to guarantee that the perturbed vectorfield $u + \epsilon\xi$ still belongs to S^2 to first order in ϵ. For all such perturbations, we easily obtain that $\int_{D^2} \langle \xi, \Delta u\rangle = 0$. Given on the one hand the restriction on ξ and, on the other hand, the freedom to choose ξ arbitrarily within this restriction, we deduce that

$$\Delta u = \mu u$$

for a scalar function μ.

To obtain μ, we proceed as follows: taking the inner product with u in the above equation and using that $||u|| = 1$, we get $\mu = \langle \Delta u, u\rangle$, and thus

$$\Delta u = \langle \Delta u, u\rangle \, u. \tag{16}$$

We re-write this equation: for $u \in S^2$, $||u|| = \sum_i {u_i}^2 = 1$, where u_i are the cartesian coordinates in $\mathbb{R}^3$ of u. Taking partial derivatives w.r.t. x_j, we see that:

$$0 = \frac{\partial}{\partial x_j} \sum_i {u_i}^2 = 2 \sum_i u_i \frac{\partial u_i}{\partial x_j}.$$

Taking derivatives w.r.t. x_j again, we get for each $j = 1, 2$:

$$\frac{\partial}{\partial x_j} \sum_i u_i \frac{\partial u_i}{\partial x_j} = \sum_i \left(\frac{\partial u_i}{\partial x_j}\right)^2 + \sum_i u_i \frac{\partial^2 u_i}{\partial {x_j}^2} = 0.$$

If we sum this over j the result is

$$|\nabla u|^2 + \langle \Delta u, u \rangle = 0, \tag{17}$$

where, still by definiton, $|\nabla u|^2 = \sum_{i,j} \left(\frac{\partial u_i}{\partial x_j} \right)^2$. So (17) holds for any C^2-mapping $u : D^2 \to S^2$. Combining (16) with (17), a harmonic map $u : D^2 \to S^2$ satisfies the following equation:

$$\Delta u + |\nabla u|^2 u = 0, \tag{18}$$

which is the right hand side of equation (1) from the Introduction.

Let us now mention some results for the radially symmetric case of (18),

$$\Lambda(\theta) \equiv \Delta\theta - \frac{\sin 2\theta}{2r^2} = 0, \tag{19}$$

with initial and boundary conditions as in problem (6)-(9). The solutions to (19) can be found by substituting $r = e^y$, multiplying the resulting equation by θ_y and integrating with respect to y, which transforms it into

$$(\theta')^2 = \sin^2 \theta + C$$

where the integration constant C turns out to be zero because of the boundary condition $\theta = k\pi$ for $r = 0$. So

$$\frac{|\mathrm{d}\theta|}{|\sin\theta|} = |\mathrm{d}y|.$$

When $\Theta = k\pi$, there is only the trivial solution $\theta \equiv k\pi$. Now let $|\Theta - k\pi| < \pi$. It follows after some computations that, in terms of r again,

$$\theta(r) = k\pi + 2\arctan\left(r \tan \frac{\Theta - k\pi}{2} \right). \tag{20}$$

But when $|\Theta - k\pi| > \pi$, it follows easily that there is no solution.

The solutions in (20) to (19) can be found using backward stereographic projection from the south pole of S^2 to the plane embedded in $\mathbb{R}^3$ in the following way (see Struwe [9], p.15).

Because of the radial symmetry, we consider only the two-dimensional cross-section of the sphere shown in figure 1. Let r on the horizontal axis be given. By backward stereographic projection one constructs the point P on S^1. P defines the angle θ (called h in this figure). One checks easily that $\theta = 2\zeta$, where ζ is the angle between the two straight lines at S in the figure. It follows that $\tan\frac{\theta}{2} = \frac{r}{2}$. Because equation (19) is invariant with respect to dilations $r \mapsto \lambda r$, $\theta(r) = 2\arctan(\lambda r)$ solves (19) as well.

Now, because (as is easy to check) the composition of a harmonic map θ satisfying (19) with a conformal map Φ is again a harmonic map Ψ, it follows that $\Psi(r) = 2\arctan(\gamma\Phi(r))$. We shall see that the equilibrium solutions to equation (10) can be written as such a composition $\theta(\Phi(r))$.

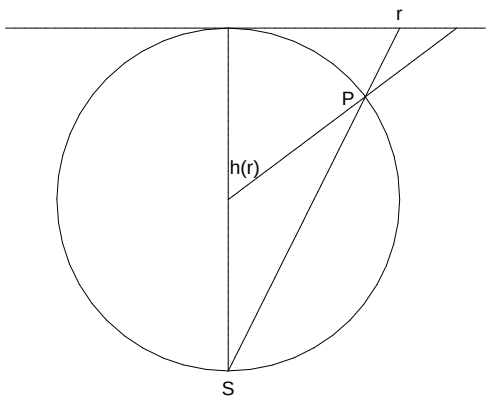

Figure 1: Given r, stereographic projection from S is used to obtain the angle $h(r)$.

2.3 The boundary conditions of problem (10)-(13); energy priciples

We still have to discuss why problem (10)-(13) would in a certain way be overdetermined by the demand that $\theta(0,0) = 0$. Let us make this precise here.

A prescription of $\theta(0,t)$ for all t would restrict the conditions under which the problem has a global solution. We shall see in what follows that (i) the requirement that some energy integral is finite restricts the possible values of $\theta(0,t)$, and (ii) that under appropriate boundary conditions, the solution to problem (10)-(13) will make a jump over $k\pi$ in $r = 0$ at a time $t = T$, thereby losing a positive amount of energy. If we would fix $\theta(0,t)$ for all t, this jump would not be possible, and we would not be able to continue the solution beyond $t = T$.

When we translate (1)-(3) into the one-dimensional system (6)-(9) using polar co-ordinates, the boundary condition at ∂D^2 translates to a boundary condition at $r = 1$ only. The situation can be compared with the Dirichlet problem on the two-dimensional disc: suppose we look for $u : D^2 \longrightarrow \mathbb{R}$ satisfying

$$\Delta u = f \quad \text{on } D^2, \tag{21}$$

$$u = 0 \quad \text{on } \partial D^2, \tag{22}$$

where $f(x) = g(r)$ for $x = (x_1, x_2) \in D^2$ is radially symmetric. If we look for a radially symmetric solution to (21) (i.e. suppose that $u(x_1, x_2) = v(r)$ with $r = \sqrt{x_1^2 + x_2^2} \in \bar{I} = [0,1]$), then the boundary condition $u = 0$ on ∂D^2 translates to $f(1) = 0$. But we need a boundary condition for $r = 0$ as well to ensure smoothness of the solution u: it is well known that v should satisfy $v_r(0) = 0$, if we want u to be smooth in $x = 0$, for u is an even function of x_1. It is necessary to add this relation as a boundary condition in the r-dependent formulation of the problem.

In our present problem (10)-(13), the boundary value at $r = 0$ is prescribed as follows: restrict the radially symmetric solution u to the x_1-axis in D^2. For x on the

positive x_1-axis we have $u(x) = (\sin\theta(x), 0, \cos\theta(x))$, for there we have $r = x$ and $\varphi = 0$. But for negative values $-x$, we have $u(-x) = (-\sin\theta(x), 0, \cos\theta(x))$. If we want the restricted solution (and consequently the solution u itself) to be smooth on D^2, the demand is that $\sin\theta(-x) = -\sin\theta(x)$, so $\sin\theta(r)$ is an odd function of r. This means that any smooth solution to (10)-(13), $\theta(r)$, should satisfy the boundary condition $\theta(0) = k\pi$ at $r = 0$.

This condition is also implied by the demand that the energy corresponding to the solution be finite (this is physically speaking the only plausible situation). Equilibrium solutions to equation (6) can be construed as solutions of the Euler-Lagrange equation corresponding to an integral, which happens to be the energy-integral in our case. Recall the following: let a functional J of the form

$$J(u) = \int_\Omega F\left(x, u(x), u'(x)\right) \mathrm{d}x, \quad \text{where } F : V \to \mathbb{R} \in C^1(V), \quad \text{and } V \subset \mathbb{R}^3, \tag{23}$$

be given. One can try to minimize this functional J over some set of functions $\mathcal{F}$, for example $\mathcal{F} = C^1([x_0, x_1])$, provided that J has a lower bound. This minimum, when it is attained at, say, $\hat{u}$, will satisfy the Euler-Lagrange equation (for the derivation and the exact conditions under which it is valid, see any textbook on the calculus of variations):

$$\frac{\mathrm{d}}{\mathrm{d}x} F_{u'}(x, \hat{u}(x), \hat{u}'(x)) - F_u(x, \hat{u}(x), \hat{u}'(x)) = 0 \tag{24}$$

However, a solution of (24) is only a stationary point of J and not necessarily a minimizer.

In the case that has our interest, where we try to minimize integral (14), we introduce in D^2 polar co-ordinates $r = \sqrt{x_1^2 + x_2^2}$, $\varphi = \arctan\frac{x_2}{x_1}$. A straightforward computation allows us to re-write (14) in terms of θ as

$$\mathcal{E}(\theta) = \pi K \int_0^1 \left(\theta_r^2 + \frac{\sin^2\theta}{r^2}\right) r \,\mathrm{d}r. \tag{25}$$

From here on, we will omit the constant πK. We are only interested in situations where the energy (25) is finite. This has the following consequences for our problem: let us consider the substitution $e^y = r$. This casts equation (6) into the following form:

$$h_t = \frac{1}{e^{2y}} \left(h_{yy} - \frac{1}{2}\sin 2h\right) \tag{26}$$

for $y < 0$, $t < T$. The equilibrium solution $h_t = 0$ to this equation is obtained by minimizing the energy integral corresponding to (25), which is given by:

$$\int_{-\infty}^0 \left(h_y^2 + \sin^2 h\right) \mathrm{d}y \tag{27}$$

The minimum $\hat{h}$ satisfies the equation for the simple pendulum. An analysis of the phase plane of the pendulum system shows that the only orbits, for which the integral

in (27) is finite, are the heteroclinic orbits that connect the saddlepoints in the phase plane. For a discussion of the simple pendulum, see any dynamical systems textbook, for example P. H. Drazin [5]. For such heteroclinic orbits, $h \to k\pi$ as $y \to -\infty$, where $k \in \mathbb{Z}$. Translated in terms of our problem, this statement becomes: $\theta \to k\pi$ as $r \to 0$.

2.4 Existence of the solution to problem (6)-(10) and blow-up results

The energy formulation is used as well in other contexts, The idea is as follows (see [7] for the details): if θ is a solution to problem (6)-(9), the energy $\mathcal{E}$ as defined in (25) may not increase in time when θ is smooth enough. This is reflected in our problem by the fact that

$$\frac{\mathrm{d}}{\mathrm{d}t}\mathcal{E}(\theta) = -\int_0^1 2r\theta_t^2 \,\mathrm{d}r \leq 0 \tag{28}$$

which one can prove using integration by parts (here one needs the smoothness of θ and its partial derivatives). The boundedness of $\mathcal{E}(\theta)$ is used to establish the existence of a limit solution $\bar{\theta}$ such that $\theta(r,t) \to \bar{\theta}$ as $t \to \infty$ in a sense made precise in [7].

Let us now define precisely what is meant by finite time blow-up:

Definition 2.1 *A mapping $u(r,t) : D^2 \times (0,T) \to S^2$ is said to blow up in finite time T if*

$$\limsup_{t \uparrow T} |\nabla u(\cdot, t)| = \infty.$$

This definition can be extended to include more general mappings between manifolds. The idea is, that blow-up occurs when the derivative at some point of the domain tends to infinity. In this way it is easy to speak of numerical blow-up, as we shall see later.

It was thought for some time that blow-up would occur only in the heat flow of harmonic maps between surfaces of dimension ≥ 3. There were various examples (see [4] for the references) of finite time blow-up. For surfaces of dimension two, there were several results on the global existence of weak solutions, for example [3].

Global existence of the solution $u(x,t)$ implies convergence to a harmonic map $\bar{u}(x)$. In our problem (1)-(3) we have the following: the energy arguments given in section 2.3 show that under appropriate boundary conditions, the limit map $\bar{u}$ has a different value at $x = 0$ than the initial condition $\psi = u(x,0)$. In combination with the fact that u may only assume a discrete set of values for $r = 0$, this means there is blow-up for all initial-boudary conditions and for all values of n; the question remains, whether the blow-up happens after a finite time T. The result by Chang, Ding and Ye [4] provided the first example of finite time blow-up of the heat flow of

mappings between manifolds of dimension 2.

To start with the existence result in [3], to which we refer the reader for the proof:

Theorem 2.2 *(Chang, Ding, [3]) If $\psi \in C^{1+\alpha}([0,1])$ is the initial condition to problem (6)-(9), and $\psi(r) \leq \pi$ for all $r \in [0,1]$, then a classical solution to this problem exists for all $t < \infty$.*

Two years later, Chang and Ding, jointly with Ye, published the first blow up result for dimension 2 in [4]. Their method was to construct a subsolution f to problem (6)-(9) that blows up in finite time. A maximum principle then forces θ to blow up in finite time. This is their result:

Theorem 2.3 *(Chang, Ding, Ye, [4]) Suppose that $\phi \in C^1(D^2, S^2)$ is radially symmetric with $\psi(0) = 0$ and $|\psi(1)| > \pi$. Then the solution $\theta(r,t)$ to problem (6) with the initial map $\psi(r)$ induced by ϕ blows up in finite time.*

We will now turn our attention to the derivation of equation (10) from problem (6).

2.5 The relation between equations (10) and (6)

Both for physical and for mathematical reasons it is interesting to consider less symmetric situations than the heat flow of harmonic maps. Mathematically, a first attempt to create a nonsymmetrical situation is the following; it will result in the derivation of equation (10):

Consider the map $F : D^2 \to D^2$ defined by $F(z) = z^n$ in complex notation, where n is an integer. We denote by ρ the radius in the domain of F and by r the radius in its range, so that $r = \rho^n$. In polar notation, $F(\rho, \varphi) = (r, n\varphi)$.

We compose the map F with $u : D^2 \to S^2$ to obtain $w = u \circ F : D^2 \to S^2$. One calculates that, for our choice of F,

$$\Delta w + |\nabla w|^2 w = |F'|^2 \left(\Delta u + |\nabla u|^2 u\right) = n^2 r^{2-\frac{2}{n}} \left(\Delta u + |\nabla u|^2 u\right). \tag{29}$$

Next, consider the solution to problem (1)-(3), but now with initial mapping

$$w_0(x) = \phi(F(x)) \tag{30}$$

for $x \in D^2$ replacing (2). Here ϕ is still the radially symmetric mapping from (2), and w_0 can be written

$$w_0(x) = (\cos n\varphi \sin \psi(\rho^n), \sin n\varphi \sin \psi(\rho^n), \cos \psi(\rho^n)).$$

We define a new problem (1), (30), with boundary conditions $w(\cdot, t)|_{\partial D^2} = w_0|_{\partial D^2}$, and call the solution $w(x,t)$. Now, if u is radially symmetric, one proves easily that Δu is radially symmetric as well, so that the right hand side of (29) is radially symmetric. Similar to the proof that the solution to (1)-(3) remains radially symmetric, one

proves now that, for each t for which $w(x,t)$ exists, there is a radially symmetric mapping $\hat{u} : F(D^2) = D^2 \to S^2$ such that $w(x,t) = \hat{u}(F(x),t)$. Now by equation (29), for this t we have

$$w_t(x,t) = \hat{u}_t(F(x),t) = n^2 r^{2-\frac{2}{n}} \left(\Delta \hat{u}(F(x),t) + |\nabla \hat{u}(F(x),t)|^2 \hat{u}(F(x),t) \right),$$

where the spatial derivatives are taken with respect to the variables in $F(D^2)$. Now that w has been translated in terms of $\hat{u}$, one writes for $F(x) = y$ in the preimage of $\hat{u}$:

$$\hat{u}_t(y,t) = n^2 r^{2-\frac{2}{n}} \left(\Delta \hat{u}(y,t) + |\nabla \hat{u}(y,t)|^2 \hat{u}(y,t) \right). \tag{31}$$

We can write now, for all t for which the solution $w(x,t)$ exists and for $x \in D^2$: there exists a function $h : [0,1] \to \mathbb{R}$ such that[4]

$$w(x,t) = (\cos n\varphi \sin h(\rho^n,t), \sin n\varphi \sin h(\rho^n,t), \cos h(\rho^n,t)). \tag{32}$$

By (31), this means for $h(r,t)$ that

$$h_t = \left(h_{rr} + \frac{h_r}{r} - \frac{\sin 2h}{2r^2} \right) n^2 r^{2-\frac{2}{n}} \tag{33}$$

After the substitution $\rho^n = r$, and then writing by abuse of notation $\theta(r,t) = h(\rho,t)$, we get equation (10) from the Introduction:

$$\theta_t = \theta_{rr} + \frac{1}{r}\theta_r - \frac{n^2 \sin 2\theta}{2r^2}.$$

For $w_t = 0$, we know that the equilibrium solution w is a harmonic mapping, for it is the composition of a harmonic with a conformal mapping. By what was said at the end of section 2.2, it follows that an equilibrium solution to (10) satisfies

$$\theta(r,t) = 2 \arctan(\lambda r^n).$$

2.6 Finite time blow-up in the case $n \neq 1$

Bertsch, Van der Hout and Vilucchi [2] improved the result in [4] (Theorem 2.3), by modifying the construction of the subsolution in such a way that it is applicable to all $n < 2$ and to a more general singularity term: they considered the problem

$$\begin{aligned} \theta_t &= \theta_{rr} + \frac{1}{r}\theta_r - \frac{g(\theta)}{r^2}, && (34) \\ \theta(r,0) &= \theta_0(r), && (35) \\ \theta(1,t) &= \Theta. && (36) \end{aligned}$$

[4]However, note that h is not the same function as θ, the solution to (6)-(9).

The function g takes a form that includes all cases $n > 0$ in equations (10) above, and it shares some properties with the sine function. Important are the properties that $g(0) = 0$ (to ensure that there is no multiple singularity in $r = 0$) and that $\int_0^A g(s)\,\mathrm{d}s \leq 0$, where A is the period of g. See [2] for the exact conditions on g. It turns out that $0 < g'(\theta) < 4$ implies that there will be blow-up for certain initial and boundary conditions. This is equivalent with saying that $n < 2$ if we take $g = \frac{1}{2}n^2 \sin 2\theta$.

The idea is still to construct a subsolution that does blow up in finite time. A crucial Proposition in the proof is the following:

Proposition 2.4 *(Bertsch, Van der Hout, Vilucchi [2]) Let $\psi(r)$ be an increasing function with $\psi(0) = 0$ and satisfying*

$$\psi_{rr} + \frac{\psi_r}{r} - \frac{g(\psi)}{r^2} = 0,$$

where $g'(0) := n^2 > 0$. Then
(i) If $n = 1$, then $0 < \psi_r(0) < \infty$;
(ii) There exists $C > 0$ such that $\psi(r) = Cr^n + o(r^n)\,(r \to 0)$.

This Proposition can be applied to analyse the behaviour of the equilibrium solutions to problem (10)-(13). Actually, it follows already from the computation of the equilibrium solution in the previous section, that these statements hold. In the proof, the Proposition helps to estimate the candidate-subsolution f. Statement (ii) will be of some importance to us in the last chapter.

We will not go deeper into the details of the proof here and refer the reader to [2]. Important for us is the result itself, and also the method used to prove the result. It depends strongly on the fact that $n < 2$, or more generally that $0 < g'(\theta) < 4$.

But if $n > 2$, global existence of the solution to (10) can be proved, as the authors of [2] also remarked. The idea is here (analogous to the previous case) to construct a supersolution that does not blow up in finite time. This is still possible in the more general problem (34) where $n^2 \sin 2\theta$ is replaced by a function $g(\theta)$. In this proof, a restriction on the initial condition has to be removed that is thought to be irrelevant.

Then $n = 2$ is the only case for which it has not been proved analytically, whether the solution to (10) exists for all time. It is expected however, on account of formal results by Van den Berg, Hulshof and King ([1]), that there is no finite time blow-up in this case. In the remaining part of this paper, we intend to say something about the case $n = 2$ numerically.

3 General remarks about numerical methods

In this chapter I will first discuss my own attempts to approximate problem (10) numerically with the goal of gaining insight into the role of the term $\frac{n^2 \sin 2\theta}{r^2}$. These attempts failed, because the methods I used were not suited for dealing with the large derivatives, that occur near $r = 0$ in the exact solution to (10).

In the second section I will give a brief outline of the so-called moving grid method for solving PDEs numerically, and discuss its virtues over fixed grid methods in our situation. For a comprehensive discussion see the dissertation of Zegeling [10].

And in the third section I will deal with the following question: is there a criterion (C), given some numerical approximation to problem (10)-(13), such that (C) is necessary and/or sufficient for the finite time blow-up (FTB) of the exact solution to (10)?

3.1 Numerical solution of problem (10)-(13) by fixed grid methods

When first dealing with the problem of finding a numerical approximation, we tried some standard techniques for solving PDEs numerically. We basically followed the Method of Lines (MOL) with a fixed spatio-temporal grid. This method is, however, not suitable at all for dealing with high-valued derivatives. If numerical blow-up is to be detected, the approximation should have many grid points in the spatial region $(0, \bar{r})$ where the derivatives to the exact solution θ are large. In practice, too much grid refinement is necessary to obtain numerical solutions that show blow-up in some sense. We shall see this in chapter 5 when discussing the output of the Zegeling code, which can also be run using a fixed grid.

The result was, that numerical blow-up was not seen in the MOL-approximation for any value of n or for any boundary value $\theta(1)$. We only saw approximations converging to an "equilibrium" that was like the arctangent-solution expected when $|\theta(r, 0)| < \pi$ and $n = 1$.

The main reason that this method fails is, that the singularity in $r = 0$ is not regularized. But the fact that the singularity causes problems for methods using a fixed grid does not mean that all such methods will fail. Different strategies for dealing with the singularity in $r = 0$ can be tried. One of these strategies is the regularization by a substitution $r \to \sqrt{r^2 + \epsilon^2}$, like in the Zegeling code.

Another possibility, which we did not consider until we obtained the Zegeling code, is to re-write the right hand side $\Lambda(\theta)$ of (10) as follows: write $\theta(r) = rh(r)$. After some computations we obtain for h:

$$h_t = h_{rr} + \frac{3h_r}{r} + n^2 \frac{2hr - \sin 2hr}{2r^3 h^3} h^3. \tag{37}$$

This equation for h has no singularity at $r = 0$, because the factor in the h^3-term is an analytic function of rh and the first two terms together form the Laplacian of a radially symmetric function h on a 4-dimensional domain.

There are more ways of re-writing problem (10)-(13), in order to make numerical computations easier, that are worth consideration. In the last two chapters, however, we only consider the ϵ-regularization. This regularization will be explained further in chapter 4.

3.2 The method of moving grids

Moving grid methods for solving PDEs numerically belong to the class of time-dependent adaptive methods. However, a special feature of moving grid methods is, that the grid is adapted continuously in time. This constitutes the difference with so-called static regridding, where we have only local grid refinement, i.e. there is only grid adaptation on a discrete set of time points. Although static regridding has the advantage over moving grid methods that it involves less computational effort per grid point, for certain types of PDEs the former method has certain drawbacks, for example the fact that numerical interpolation must be used to transfer information from old to new grid points.

Moving grid methods use less time steps and less space steps; in fact, they may use only a fixed (and relatively small) number of space steps. The density of grid points is highest where spatial-temporal gradients of the solution are large.

3.3 What conclusions concerning blow-up can possibly be drawn from the numerical output?

Suppose that one has some output of a numerical scheme that seems to blow up in finite time under certain conditions. Is there any way, given the original problem (P), the numerical scheme and the conditions under which blow-up seems to occur numerically, to conclude that the exact solution v to (P) blows up in finite time under the same conditions? This is the question we were concerned with when applying numerical schemes to problem (10)-(13), where we found numerical solutions that seemed to have blown up in finite time.

For our problem (10)-(13), with numerical solution $u(x_m, t_i)$, one would also expect that the blow-up behaviour of the exact solution is approached in some way as we refine the grid. Let us consider the following criterion:

Definition 3.1 • *If after some time t_i the numerical solution u satisfies $|u(x_0, t_i) - \pi| < \eta$, where x_0 is the spatial grid point corresponding to $r = 0$, we conclude that the*

exact solution $\theta(r,t)$ has blown up before $t_i + \delta$, where $\delta = \delta(\eta)$.
• *If the numerical solution satisfies $|u(x_0,t_i)| < \eta$ for all $t_i < TF$ (the final time of the numerical computations), we conclude that the exact solution $\theta(r,t)$ does not blow up in finite time.*

We will say that an approximation that satisfies criterion (3.1) has numerical blow-up. But are we justified in inferring FTB of the exact solution θ corresponding to the approximation u? A difference between the exact and the numerical situation is, that the exact solution θ can only assume the discrete set of values $\{k\pi,\ k \in \mathbb{Z}\}$, while the numerical solution that we shall define in chapter 5 can assume all possible values for $x_0 = 0$.

Example 3.1

We considered the following simple model:

$$\frac{\mathrm{d}v}{\mathrm{d}t} = v^{1+\epsilon}; \qquad v(0) = v_0. \tag{38}$$

Our aim was to see whether in this model finite time blow-up of the exact solution could be inferred from a numerical blow-up criterion like 3.1. Equation (38) blows up in finite time when ϵ is positive, and for $t = \infty$ when $\epsilon = 0$. The solutions are given by

$$v(t) = (v_0^{-\epsilon} - \epsilon t)^{-\frac{1}{\epsilon}}$$

with finite blow-up time (BUT) $(\epsilon\, v_0^{\epsilon})^{-1}$ and in the limit case $\epsilon = 0$, of course, $v(t) = v_0\, e^t$. From now on, we shall call $v(t) = v(\epsilon;t)$ and assume that $v_0 = 1$. Note that in this particular case we have

$$\lim_{\epsilon \to 0} v(\epsilon;t) = v(0;t).$$

Although we know what happens in the exact situation here, we can compare the behaviour of the exact solution to that of the following Euler approximation:

$$\begin{cases} u_{n+1} = u_n + h_{n+1} u_n^{1+\epsilon} = u_n + h_{n+1} u'_n, \\ h_{n+1} u'_n = \text{constant}. \end{cases}$$

Here $u_n = v(t_n)$ is the approximation to v at time $t_n = \sum_{j=1}^{n} h_j$, where the stepsize is variable and determined after each integration step by the simple demand that $h_{n+1}u'_n$ be constant, so that we actually have

$$h_{n+1} = \frac{h}{u'_n},$$

where $h = h_1$ is the initial stepsize and $v(0)$ is supposed to be equal to 1. Now the numerical solution is simplified to

$$u_n = u_0 + nh.$$

This ensures that $u_n \to \infty$ as $n \to \infty$. The question whether the approximation blows up in finite time is then reduced to the question whether the following series (which gives the numerical *BUT*) converges to some finite number:

$$\sum_{n=0}^{\infty} h_{n+1} = \sum_{n=0}^{\infty} \frac{h}{(nh)^{1+\epsilon}}.$$

This is the case for this particular equation (by the integral criterion). However, for $\epsilon = 0$ this sum reduces, as the reader can check, to

$$\sum_{n=0}^{\infty} h_{n+1} = \sum_{n=0}^{\infty} \frac{1}{n},$$

which is a divergent series, of course. Note that the criterion for numerical blow-up was already implied by the numerical method used.
□

It seems, therefore, that we have found a criterion to determine by a numerical approximation whether or not the exact solution blows up in finite time. For in a more general setting we could study the problem

$$u' = f(u); \qquad u(0) = u_0. \tag{39}$$

Applying the above Euler method would lead us to determining whether the integral

$$\int_{\delta}^{\infty} \frac{\mathrm{d}u}{f(u)}$$

converges for $0 < \delta \in \mathbb{R}$, by the same arguments as above (as the reader can check). So because of the equivalence of the convergence of the integral and that of the sum, we can prove the following Theorem:

Theorem 3.2 *Let f be a monotonically increasing and positive real function defined on [0,∞) and let $u_t = f(u), \qquad u(0) = u_0 > 0$ be the ODE defined by f. Let this equation be approximated by the Euler method described above, where the stepsize is determined by the demand that $u'_n h_{n+1}$ be constant. Then the following two situations are equivalent:*
(a) The exact solution to (39) blows up for $t = T$; and
(b): The approximation to (39) blows up for $t = T_N$.

Proof:
We will prove that, for finite M,

$$(a) \Longleftrightarrow \int_{u_0}^{\infty} \frac{\mathrm{d}u}{f(u)} = M \Longleftrightarrow (b).$$

We know that, for equation (39),

$$\int_{u(0)}^{u(t)} \frac{\mathrm{d}u}{f(u)} = t.$$

Moreover, because $f(u) \geq c > 0$, $u(t) \to \infty$ as t grows large enough.

Suppose now that $u(t) \to \infty$. Then $t \to M < \infty$. It is easy to see now, that the implication holds the other way around as well. This proves the first equivalence of assertion (a) and our supposition.

The supposition that the above integral be finite is also equivalent, as was shown preceding the Theorem, to the convergence of the sum for the BUT (by the integral criterion). This proves the equivalence of (a) and (b).
□

It is easy to show that $T_N > T$, T_N depends on the initial stepsize h, and $T_N \to T$ as h tends to zero.

However, when one approximates the solution to some problem, the behaviour of the exact solution is usually unknown. For problem (10)-(13) this is also the case. So what is the use of the above exposition, if we can never be sure that our approximation conserves the blowing up behaviour of the exact solution? Its use is, that it may indicate what kind of approximation preserves the FTB-property, and that, secondly, that there *are* in fact cases of numerical schemes preserving such delicate properties as FTB. The FTB-property is delicate because it requires control of the stepsize and it requires taking into account very large derivatives in the spatial as well as in the temporal variables. These requirements are fulfilled by the Zegeling scheme. (However, as we shall see in chapter 5, it is difficult to find a numerical blow up criterion that works in the cases where the exact solution is known.)

On the other hand, the ODE-scheme analysed in this paragraph is incomparable to our parabolic PDE in several ways. The dependence on several variables will make numerical calculations much more difficult in the PDE case. As a second difference, the kind of blow-up is different: for the simple ODE-scheme, blowup means that the solution tends to infinity, while for our equation it means that some derivative tends to infinity (namely the spatial derivative at r=0). This is a condition which is impossible to verify for the numerical solution. Still, Zegelings code shows numerical blow-up, as we shall see. We shall look for an explanation of this numerical blow-up in the conservation of some energy associated with the equation, among other things.

Another interesting suggestion for a numerical blow-up criterion can be found in an article by D. Estep, titled "Preservation of invariant domains under discretization" [6]. It concerns numerical approximation of problems with blow-up. The author states that for such problems, before the question whether an approximation converges or

has certain stability properties can be answered, one should ask whether we can "trust" the numerical approximation at all with regard to blow-up. He then discusses two questions: can discretization prevent blow up (i.e., the numerical solution does not blow up in finite time while the exact solution does); and can it cause "artificial" blow-up (i.e., the exact solution does not blow up but the numerical solution does)? Although Estep investigates another kind of parabolic equation with another type of blow-up than we do here, these two questions are precisely what concerns us in this section.

Regarding the first question, Estep poses that blow-up can only be "prevented" if the numerical solution is too inaccurate. In other words: accurate numerical solutions preserve the FTB-property. However, from the simulations that we will present in chapter 5, this is doubtful. The second question is dealt with by Estep in more detail: the criterion he proposes is a statement about invariant regions. Recall that an invariant region for a time-dependent problem is a subset of the solution space such that, once the solution enters this subset for $t = t_1$, the solution will stay in this subset for all $t > t_1$. If a scheme preserves invariant regions belonging to the equation, then blowup will most probably not occur in the approximation when it is not seen in the exact solution. So he states ([6]):

If blow-up is seen in a numerical solution that preserves invariant regions, this is strong evidence that blow-up is occurring.

To conclude this (rather enquiring) section: what can we expect, then, of a numerical approximation, when we are interested in deciding whether FTB occurs in equation (10)? We saw that there exist criteria suggesting that the numerical approximation *can* preserve the FTB-property of the exact solution. However, our problem is quite different from these cases.

But there is another way of characterizing the blow-up of θ: we can see if the numerical solution conserves the energy.

4 Zegeling's moving grid scheme: a description and a justification of its use

The code we received from Dr. Paul Zegeling (Utrecht University) allowed us to obtain some interesting numerical data. It is about these data and their interpretation that the remaining part of this paper will be. In the present chapter the numerical scheme will be introduced, and we will examine the relation between the scheme and problem (10)-(13). In chapter 5, the output will be demonstrated and interpreted using the results of this chapter. Central in both remaining chapters is the question, whether the numerical blow-up that is seen in the output tells us anything about FTB in the exact solution to (10)-(13).

The Zegeling-code can solve (10)-(13) either by so-called moving grid methods or by a method approximating on a fixed grid. The code has been applied to a wide range of problems already, among which (quite recently) the Gray-Scott equation. In order to compute approximations to the solution θ of problem (10)-(13), the Zegeling code was applied to the following regularization of (10)-(13):

$$\theta_t = \theta_{rr} + \frac{\theta_r}{\mathrm{sgn}(r)\sqrt{r^2+\epsilon^2}} - n^2 \frac{\sin 2\theta}{2(r^2+\epsilon^2)} \quad \text{for} \quad (r,t) \in (-1,1)\times(0,T); \tag{40}$$

$$\theta(r,0) = \theta_0(r) \quad \text{for} \quad r \in [-1,1]; \tag{41}$$

$$\theta(-1,t) = \theta(1,t) = \theta_0(1) = \Theta \quad \text{for} \quad t < T. \tag{42}$$

For a transparent notation, we will use from now on the notation θ_ϵ (with subscript ϵ) to denote solutions to problems or equations where the regularization $r \to \sqrt{r^2+\epsilon^2}$ has been applied. Note that in (40) we did not only regularize the singularity in $r = 0$, but that we also changed the domain of r to $[-1,1]$. The reason for the domain enlargement is, that the numerical scheme needs a second boundary condition, which is now supplied for $r = -1$. We will analyse in the following sections what are the consequences of these two adaptations for the blow-up behaviour of θ_ϵ.

4.1 Two problems in justifying the use of the Zegeling scheme

As we have seen, the Zegeling code computes an approximation to problem (40)-(42). This problem differs from problem (10)-(13) in its domain as well as in the equation. When we apply the code to problem (10)-(13) and interpret the numerical output, we have to see first of all that an exact solution $\theta_\epsilon(r,t)$ to the problem approximated, (40)-(42), can be restricted to the original domain $[0,1]\times(0,T)$, such that the restriction $\theta_\epsilon|_{(0,1)\times(0,T)}$ tends, as $\epsilon \to 0$, in some way to $\theta(r,t)$, the solution to problem (10)-(13).

The initial function ψ, and with it at each $t < T$ the solution to (10)-(13), $\theta(r,t)$, can be extended on $[-1,0)$ either symmetrically or skew-symmetrically. The Zegeling

code uses as a default a symmetric boundary condition at $r = \pm 1$, so consider a symmetrical extension first. Let us restrict our attention to the domain enlargement for the time being, and consider the following problem:

$$\phi_t = \phi_{rr} + \frac{1}{r}\phi_r - \frac{n^2 \sin 2\phi}{2r^2} \quad \text{for} \quad (r,t) \in (-1,1) \times (0,T), \tag{43}$$

$$\phi(r,0) = \psi(r) \quad \text{on} \quad [-1,1], \tag{44}$$

$$\phi(\pm 1, t) = \psi(1) \quad \text{for} \quad t < T. \tag{45}$$

Take $\psi(r)$ as defined in (11) and extend it symmetrically by putting $\psi(-r) = \psi(r)$. Then, by an easy computation, $\phi_t(r,t) = \phi_t(-r,t)$ for all $r \in (-1,1)$ and $t < T$. So $\phi(r,t)$ will be symmetric around $r = 0$ for $t < T$ as well:

$$\phi(r,t) = \phi(-r,t) \text{ for all } r \in (-1,1),\ t < T.$$

By the same considerations as in problem (10)-(13), we still have $\phi(0,t) = k\pi$ for $t < T$. So

$$\phi|_{[0,1]\times[0,T)} = \theta \text{ on } [0,1] \times [0,T).$$

A problem with this symmetric extension of the solution around $r = 0$ is, that $\theta_r(0,t)$ may be nonzero in problem (10)-(13), and that $\phi_r(0,t)$ cannot.

We can get rid of this inconvenience by extending ψ skew-symmetrically around $r = 0$, and adapting the left boundary condition as well to $\phi(-1,t) = -\psi(1)$. The problem defined by these adaptions will be called (43^a)-(45^a), and its solution will be called $\hat{\phi}$. We define (40^a)-(42^a) similarly, with solution $\hat{\theta}_\epsilon$. Then $\hat{\phi}$ satisfies $\hat{\phi}_t(r,t) = -\hat{\phi}_t(-r,t)$ on all of its domain, so it is skew-symmetric as well. For the restriction, $\phi|_{[0,1]\times[0,T)} = \theta$ holds again. The advantage is now obviously that the derivative $\phi_r(0,t)$ is well-defined, but this is only the case for $t < T$. After the blow-up time T (if there is one) $\hat{\phi}(r,t)$ cannot be defined as a continuous solution. But this is only a minor problem, because $\sin\hat{\phi}$ will be continuous for $r \in [-1,1]$. The enlargement of the domain in problem (43^a)-(45^a) does not prevent the FTB that was proved for problem (10)-(13).

This minor problem is, however, only a problem for the exact solution to (43^a)-(45^a). If θ_ϵ solves (40)-(42), then one checks that, again, $(\theta_\epsilon)_t(r,t) = (\theta_\epsilon)_t(-r,t)$. The problem with θ_ϵ is again, that $(\theta_\epsilon)_r(0,t) = 0$ for $t < T$. In the case of problem (40^a)-(42^a),

$$\theta_t = \theta_{rr} + \frac{\theta_r}{\operatorname{sgn}(r)\sqrt{r^2+\epsilon^2}} - n^2 \frac{\sin 2\theta}{2(r^2+\epsilon^2)} \quad \text{for} \quad (r,t) \in ((-1,0)\times(0,1)) \times (0,T), \tag{46}$$

$$\theta(r,0) = \theta_0(r) \quad \text{for} \quad r \in [-1,0) \cup (0,1]; \tag{47}$$

$$-\theta(-1,t) = \theta(1,t) = \theta_0(1) = \Theta \quad \text{for} \quad t < T; \tag{48}$$

$$\theta(0,t) = 0 \quad \text{for} \quad t < T, \tag{49}$$

the solution $\hat{\theta}_\epsilon$ remains skew-symmetric for all $t < T$, and we expect that the discontinuity in $r = 0$ will not disturb the numerical approximations. Remark that (46)-(49) is a more logical regularisation of (10)-(13) than (40)-(42), in the sense of the remarks about the oddness of $\sin\theta$ made in section 2.3. However, the code we received from Zegeling computed approximations to problem (40)-(42). We did not have time to adapt the code to be applicable to problem (46)-(49) as well.

A second question we have to pose is:

Question 4.1 *Is there FTB of θ_ϵ, in the sense of defenition 2.1, for any ϵ? Or does a global solution to (40)-(42) exist? And if such a global solution exists, do we have $\theta_\epsilon \to \theta$ as $\epsilon \to 0$ in some way?*

Before we try to answer this question, first the following notation. Like in the non-regularized case, steady states of (40)-(42) admit a variational formulation as well. When we define the "energy" as

$$\mathcal{E}_\epsilon(\theta) = \int_{-1}^{1} F(r) \left(\theta_r^2 + \frac{n^2 \sin^2\theta}{r^2 + \epsilon^2} \right) \mathrm{d}r, \tag{50}$$

where $F : [-1, 1] \to \mathbb{R}$ is defined as

$$F(r) = e^{-\int_{|r|}^{1} \frac{ds}{\sqrt{s^2+\epsilon^2}}} = \frac{|r| + \sqrt{r^2 + \epsilon^2}}{1 + \sqrt{1 + \epsilon^2}},$$

the Euler-Lagrange equation corresponding to (50) reads[5]

$$\theta_{rr} + \frac{\theta_r}{\sqrt{r^2 + \epsilon^2}} - \frac{n^2 \sin 2\theta}{2(r^2 + \epsilon^2)} = 0. \tag{51}$$

So a minimizer of (50) solves (51). We shall call a solution of (51) $\bar{\theta}_\epsilon$, and it is a limit solution for problem (40)-(42). It is easy to check that the energy corresponding to θ_ϵ is, like in the case $\epsilon = 0$ (see equation (28)), decreasing in time:

$$\frac{\mathrm{d}}{\mathrm{d}t}\mathcal{E}_\epsilon(\theta_\epsilon) = -2 \int_{-1}^{1} F(r)(\theta_\epsilon)_t^2 \, \mathrm{d}r \leq 0. \tag{52}$$

One would like to know, whether the limit solution $\bar{\theta}_\epsilon$ has $\bar{\theta}_\epsilon(0) \approx k\pi$, where $k = K$ or $K+1$, when $\Theta \in (K\pi, (K+1)\pi)$. We will try to answer this question in section 4.3.

In the next sections we shall examine (after Dekkers and Van der Hout [8]) the so-called semi-discrete problems corresponding to (10)-(13) and to (40)-(42). Instead of an answer to Question 4.1, which does not appear to be easily found, it would also be interesting to prove whether the solution to the semi-discrete problem blows up, and under what conditions. Such a result will be helpful in interpreting the numerical approximations to (40)-(42).

[5] $F'(r)$ is only defined for $r \neq 0$. So the Euler-Lagrange equation (51) can only be derived for those values of r. However, this problem is removed, because the limits of $\bar{\theta}_\epsilon$, as $r \uparrow 0$ and $r \downarrow 0$ respectively, are equal. Thus $\bar{\theta}_\epsilon(0)$ is well defined.

4.2 The semi-discrete problem and its FTB-behaviour

The following observation was made by Van der Hout and Dekkers [8]; we will formalize their argument here. They considered the semi-discrete problem, to find $\theta(r, t_{i+1})$ given the equation

$$\frac{\theta(r, t_{i+1}) - \theta(r, t_i)}{h_i} = \Lambda(\theta(r, t_{i+1})), \tag{53}$$

where $h_i > 0$ is the timestep, $\theta(r, t_i)$ is a known real-valued function of r after i time-steps, and $\theta(1, t_{i+1}) = \Theta \in (m\pi, (m+1)\pi)$ for some $m \in \mathbb{Z}$ is the boundary condition. Λ is the operator used for abbreviation of the right hand side of (10). From here on, we will call $\theta(r, t_{i+1}) = \theta_{i+1}(r)$. Solving this implicit problem for $\theta_{i+1}(r)$ (and doing this for several t_i) is one possible way of approximating the parabolic problem (40)-(42).

Given an initial solution $\theta_0(r) = \theta(r, 0)$, equation (53) defines a sequence $\{\theta_i\}$, where $t_i = \sum_i h_i$. This sequence is well-defined, because the energy-minimizing solution to problem (53) is unique for appropriate choices of h_i. We shall see now why this is the case.

An application of the Euler-Lagrange formalism shows that finding θ_{i+1} given θ_i can be done by minimizing the integral

$$\mathcal{E}_{\theta_i}(\theta) = \int_0^1 \left(\frac{(\theta - \theta_i)^2}{h_i} + \theta_r^2 + \frac{\sin^2 \theta}{r^2} \right) r \, \mathrm{d}r \tag{54}$$

over the set $W = \{\theta \in \mathcal{W} : \theta(1) = \Theta\}$. $\mathcal{W}$ is the Hilbert space defined in [7], section 3. If this minimum is attained at, say, θ_{i+1}, then this θ_{i+1} is a (weak) solution of equation (53). In [7], Theorems 3.7 and 3.8, the existence of a minimizer $\bar{\theta}$ to $\mathcal{E}$ is proved, such that the minimizing sequence $\{\theta_j\}$ converges weakly to this minimizer along a subsequence in $H^1(R, 1)$, for arbitrary $0 < R < 1$. We remark that the existence proof can be mimicked[6] for $\mathcal{E}_{\theta_i}$; we will prove the uniqueness of the minimizer to $\mathcal{E}_{\theta_i}$ now, provided that the timestep is appropriately small:

Proposition 4.1 *For h_i sufficiently small, there exists a unique minimizer of $\mathcal{E}_{\theta_i}(\theta)$ over W.*

Proof: Let us assume that two different minimizers of $\mathcal{E}_{\theta_i}(\theta)$ over W exist, and call them $\bar{\theta}_{i+1}$ and $\bar{\psi}_{i+1}$. Then both minimizers satisfy the semi-discrete equation (53). Thus their difference $\bar{\theta}_{i+1} - \bar{\psi}_{i+1}$ should satisfy

$$\frac{\bar{\theta}_{i+1} - \bar{\psi}_{i+1}}{h_i} = \Delta(\bar{\theta}_{i+1} - \bar{\psi}_{i+1}) - \frac{\sin 2\bar{\theta}_{i+1} - \sin 2\bar{\psi}_{i+1}}{2r^2}.$$

Let us call $f = \bar{\theta}_{i+1} - \bar{\psi}_{i+1}$. After multiplication by rf and integration over $r \in (0, 1)$, the following should hold:

[6] It is not the case, in general, that the minimizer is in W, because W is not a Hilbert space.

$$\int_0^1 r\frac{f^2}{h_i}\,\mathrm{d}r = \int_0^1 rf\Delta f\,\mathrm{d}r - \int_0^1 rf\frac{\sin 2\bar{\theta}_{i+1} - \sin 2\bar{\psi}_{i+1}}{2r^2}\,\mathrm{d}r. \tag{55}$$

Of this integral equation, the left hand side is positive for all values of h_i. We shall show that when h_i is sufficiently small, say $h_i < \bar{h}$, the equality in (55) cannot hold unless $f = 0$, which contradicts our assumption. Out of this contradiction for small h_i, uniqueness follows.

We now construct such an $\bar{h}$. The first term on the right of (55) is negative, since it can be rewritten after integrating by parts as follows (using that $f(1) = 0$):

$$\int_0^1 rf\Delta f\,\mathrm{d}r = -\int_0^1 rf_r^2\,\mathrm{d}r.$$

And the second term can be estimated as follows: Define the fixed number $r_i := \inf\{r \in (0,1)\colon \theta_i(r) \geq \frac{\pi}{4}\}$. We know that for $h_i \to 0$, the minimizers of (54) converge to θ_i uniformly on $[R,1]$, where R is arbitrarily close to zero. Moreover, it is impossible for a minimizer $\bar{\theta}_{i+1}$ to (54) that $\bar{\theta}_{i+1}(0) = k\pi$ for $k \neq 0$ when h_i is sufficiently small, because for such h_i, θ_i would be a better minimizer than $\bar{\theta}_{i+1}$.

Thus one derives the following: when $\bar{h}$ is chosen sufficiently small, then for all $h_i < \bar{h}$, we have $\bar{\theta}_{i+1}(r)$, $\bar{\psi}_{i+1}(r) < \frac{\pi}{4}$ for all $r \in (0,\bar{r})$, where $\frac{r_i}{2} < \bar{r} < r_i$ is a fixed number independent of the choice of $h_i < \bar{h}$. Then we have, still for $h_i < \bar{h}$:

$$-\int_0^{\bar{r}} rf\frac{\sin 2\bar{\theta}_{i+1} - \sin 2\bar{\psi}_{i+1}}{2r^2}\,\mathrm{d}r < 0,$$

because f has the same sign as $(\sin 2\bar{\theta}_{i+1} - \sin 2\bar{\psi}_{i+1})$ for all $r \in (0,\bar{r})$; and we also have

$$\left|-\int_{\bar{r}}^1 rf\frac{\sin 2\bar{\theta}_{i+1} - \sin 2\bar{\psi}_{i+1}}{2r^2}\,\mathrm{d}r\right| \leq \int_{\bar{r}}^1 r|f|\frac{|\bar{\theta}_{i+1} - \bar{\psi}_{i+1}|}{r^2}\,\mathrm{d}r,$$

which is smaller than the left hand side of (55) for $h_i \leq \bar{h}$. So for this choice of h_i, we have uniqueness.
□

From now on, we shall take a fixed timestep $h_i = h$. The element θ_j of the sequence $\{\theta_i\}$ may be no longer uniquely determined, and it is constructed now by choosing, if necessary, some minimizer of (54) given this fixed h. We then have the following estimates:

Proposition 4.2 *For any sequence $\{\theta_i\}$, constructed by the above algorithm (53), (54), we have the following estimates on the energies:*

$$\mathcal{E}_{\theta_{i-1}}(\theta_i) \leq \mathcal{E}(\theta_{i-1}) \leq \mathcal{E}_{\theta_{i-2}}(\theta_{i-1}) \leq \mathcal{E}(\theta_{i-2}). \tag{56}$$

Proof: Because θ_i is a minimizer for $\mathcal{E}_{\theta_{i-1}}$, we have $\mathcal{E}_{\theta_{i-1}}(\theta_i) \leq \mathcal{E}_{\theta_{i-1}}(\theta_{i-1}) \leq \mathcal{E}(\theta_{i-1})$, which proves the first inequality. The second inequality follows easily from the definitions of the functionals.
□

Moreover (see [7], Section 3 and in particular Theorem 3.7, for the details) there exist a subsequence θ_{i_k} and a continuous function $\bar{\theta}$ such that the convergence of θ_{i_k} to $\bar{\theta}$ is uniform on compact sets $[R, 1]$, where R denotes any real number in $(0, 1)$, and weak in the Hilbert space $H^1(R, 1)$. $\bar{\theta}$ is in $H^1(R, 1)$. It follows easily that $\bar{\theta}$ is a weakly harmonic map[7] and it is smooth.

Now we are ready to prove the following statement for the semi-discrete problem:

Theorem 4.3 *Let us assume, without loss of generality, that $m = 1$, i.e. $\Theta \in (\pi, 2\pi)$. Assume as well that $\theta_0(0) = 0$. Then there is finite time blow-up for the semi-discrete problem, i.e. there exists $N \in \mathbb{N}$ and a subsequence $\{\theta_{i_k}\}$ such that $k > N$ implies that $\theta_{i_k}(0) \geq \pi$, while for $k \leq N$, $\theta_{i_k}(0) = 0$.*

Proof: Note that, given the boundary condition Θ, the value at $r = 0$ of the harmonic map $\bar{\theta}$ is almost uniquely determined (it is π or 2π, or more generally, when $\Theta \in (k\pi, (k+1)\pi)$, it is $k\pi$ or $(k+1)\pi$). Now we suppose for a contradiction that $\theta_{i_k}(0) = 0$ for all k. (In principle, this could hold, because the convergence $\theta_{i_k} \to \bar{\theta}$ is only uniform on compact sets $[R, 1]$ with $R > 0$.)

This assumption implies, as $\theta_{i_k} \to \bar{\theta}$, that $r_k = \inf\{\bar{r} : \theta_{i_k}(r) \geq \pi \text{ for all } r \geq \bar{r}\}$ approaches zero as $k \to \infty$. It follows from the definition of r_k and of the subsequence θ_{i_k}, that the integral

$$\int_0^{r_k} \frac{\left(\theta_{i_k} - \bar{\theta}\right)^2}{h} r \, \mathrm{d}r$$

tends to zero as well for $k \to \infty$. But we also have the inequality (from [7], Lemma 3.11)

$$\int_0^{r_k} \left((\theta_{i_k})_r^2 + \frac{\sin^2 \theta_{i_k}}{r^2} \right) r \, \mathrm{d}r \geq 4, \tag{57}$$

whereas

$$\int_0^{r_k} \left(\left(\bar{\theta}\right)_r^2 + \frac{\sin^2 \bar{\theta}}{r^2} \right) r \, \mathrm{d}r \to 0$$

as $k \to \infty$. But for such k,

$$\int_{r_k}^1 \left(\frac{(\theta_{i_k+1} - \theta_{i_k})^2}{h_i} + (\theta_{i_k+1})_r^2 + \frac{\sin^2 \theta_{i_k+1}}{r^2} \right) r \, \mathrm{d}r \to \int_{r_k}^1 \left(\frac{(\bar{\theta} - \theta_i)^2}{h_i} + \bar{\theta}_r^2 + \frac{\sin^2 \bar{\theta}}{r^2} \right) r \, \mathrm{d}r,$$

[7]We slightly abuse the definitions here: actually, only the mapping $\bar{u}$ corresponding to $\bar{\theta}$ by equation (5) can be called harmonic, and it is smooth because D^2 is two-dimensional.

and a contradiction arises because $\bar{\theta}$ will be a better minimizer for the energy $\mathcal{E}_{\theta_{i_k}}$ than θ_{i_k+1}. This refutes the assumption that $\theta_{i_k}(0) = 0$ for all k, and consequently there exists an N such that for $k > N$, $\theta_{i_k}(0) \geq \pi$.
□

As the reader can check, exactly the same argument can be applied to equations (10)-(13), with the factor n^2 added before the last term. This means that at appropriate boundary conditions ($\Theta \notin ((k-1)\pi, (k+1)\pi)$ when $\theta(0,0) = k\pi$) and for any fixed timestep h, the semi-discrete problem will jump in $r = 0$ after a finite number of steps. The cases in which there is blow-up in a finite number of steps can be compared with the blow-up results by [4], [3], [2] and [1]. This comparison is made in the following table. We still assume in this table that $\theta(0,0) = 0$. "Y" stands for "yes" (there is FTB) and "N" for "no" (there is no FTB); "?" indicates that the blow-up behaviour is unknown. The first Y/N is for the solution to (10)-(13), the second Y/N for solutions to the semi-discrete problem.

	$\theta(1,0) > \pi$	$\theta(1,0) = \pi$	$\theta(r,0) < \pi$
$n = 1$	Y—Y	N—Y	N—N
$n \in (1,2)$	Y—Y	N—Y	N—N
$n = 2$	?—Y	?—Y	N—N
$n > 2$	N—Y	N—Y	N—N

We can conclude that this (semi-discrete) numerical method corresponding to (10) is accurate as regards the spatial derivatives, and it does *not* preserve the FTB behaviour of problem (10) in many cases. A positive thing to conclude is, that we have actually *proved* that this numerical scheme blows up after a finite number of steps (when the data are appropriate). For a moving grid method, things are more complicated: such a method amounts to solving two or more coupled PDEs (where one of those PDEs is for determining the grid), and the spatial and the temporal numerical integration cannot be separated (they are separated in the semi-discrete problem).

For this reason, the results for the semi-discrete problem are not directly applicable to the output of the Zegeling method. A second reason for this is, that the Zegeling method approximates problem (40) with $\epsilon \neq 0$. For $\epsilon \neq 0$, it is difficult to speak of blow-up in the semi-discrete problem. There is no sharp distiction between
(i) a semi-discrete sequence corresponding to an exact solution increasing continuously in $r = 0$ as time increases, and
(ii) a semi-discrete sequence corresponding to an exact solution that has FTB in $r = 0$.
We could not disprove that a solution $\theta_\epsilon(r,t)$ to (40) can in principle assume all real values for $r = 0$. There is no restriction from the energy, at least. This means also, that we cannot prove easily if $r_k \to 0$, with r_k as defined in Theorem 4.3.
In chapter 5 it will turn out that there is a third reason why it is difficult to apply the semi-discrete results to the output.

In the next section, we will analyse the semi-discrete problem for $\epsilon \neq 0$, and we shall see that the argument for $\epsilon = 0$ cannot be repeated. However, we *can* show for $\{\theta_{\epsilon,i}\}_{i=0}^{\infty}$ the solution to the semi-discrete problem for $\epsilon \neq 0$, that $\theta_{\epsilon,i}(0) \to k\pi \pm \eta$ for some small η and under certain conditions. This means that the solution blows up according to our definition 3.1 for numerical blow-up. The conditions for this numerical blow-up have to do with the convergence of r_k to zero.

4.3 Limit solutions in the case $\epsilon \neq 0$

In the case $\epsilon = 0$ we needed some properties of the *known* limit solution $\bar{\theta}$ to establish convergence of the minimizing sequence $\{\theta_i\}$ to this limit. However, we cannot solve equation (51) directly to obtain the limit solution $\bar{\theta}_\epsilon$, like in the case $\epsilon = 0$, but we can prove its existence and some of its properties by variational arguments. This is done as follows: Consider the set $W := \{x \in W^{1,2}(0,1)\}$, equipped with the following inner product $\langle \cdot, \cdot \rangle$:

$$\langle \theta_1, \theta_2 \rangle := \int_0^1 F(r) \left(\frac{\theta_1 \theta_2}{r^2 + \epsilon^2} + \theta_1' \theta_2' \right) \mathrm{d}r,$$

where $F(r)$ is defined as in (50). It is now trivial to see that W is a Hilbert space: the inner product $\langle u, v \rangle$ exists for all functions u, $v \in W$ and the norm $|| \cdot ||_W$ that it induces is equivalent to the standard norm on $W^{1,2}$.

It is important to note that $\theta \in W$ is only defined on $[0,1]$, whereas the solutions to equation (40) and the minimizers of $\mathcal{E}_\epsilon$ are defined for $r \in [-1,1]$. We consider $\theta \in W$ here, because this allows us to prove a statement about $\bar{\theta}_\epsilon(0)$. For convenience, we shall call the new energy functional

$$\mathcal{E}_\epsilon(\theta) = \int_0^1 F(r) \left(\theta_r^2 + \frac{n^2 \sin^2 \theta}{r^2 + \epsilon^2} \right) \mathrm{d}r, \tag{58}$$

defined only for $\theta : [0,1] \to \mathbb{R}$, $\mathcal{E}_\epsilon$ as well. By the symmetry and the skew-symmetry around $r = 0$ of the solutions to problems (40)-(42) and, respectively, (46)-(49), the results we are going to prove for $\theta \in W$ hold as well for limit solutions $\bar{\theta}_\epsilon : [-1,1] \to \mathbb{R}$ to these problems.

The above integral (58) is finite for all $\theta \in W$. We will minimize $\mathcal{E}_\epsilon$ over $\{\theta \in W : \theta(0) = \alpha; \theta(1) = \Theta\}$, where $\alpha \in \mathbb{R}$. Let a minimizing sequence for $\mathcal{E}_\epsilon$ be $\{\theta_i\}$. Such a sequence exists because $\mathcal{E}_\epsilon$ is bounded from below by 0.

Proposition 4.4 *The sequence $\{\theta_i\}$ converges weakly in W to some limit $\bar{\theta}$.*

Proof: To prove this Proposition, we first consider the sequence $\{\zeta_i\}$, where $\zeta_i(r) = \theta_i(r) - \Theta$, and show that it is bounded in W. On the set $W^* = \{\zeta \in W \text{ such that } \zeta(1) = 0\}$, the following is a norm:

$$||\zeta||_* = \sqrt{\int_0^1 (\zeta')^2 \, \mathrm{d}r}. \tag{59}$$

The ζ_i are bounded with respect to $||\cdot||_*$, on account of the inequality

$$||\zeta_i||_*^2 \leq \mathcal{E}_\epsilon(\theta_i) \leq M,$$

where the last inequality is due to the fact that $\{\theta_i\}$ was a minimizing sequence for $\mathcal{E}_\epsilon$ in W. The first inequality follows easily from the definitions. We now show that

Lemma 4.5 *$||\cdot||_*$ is equivalent to the norm $||\cdot||_W$ induced by the inner product $\langle\cdot,\cdot\rangle$.*

Proof: We have the estimates, for $\theta \in W^*$ and real constants A_1 and A_2,

$$||\theta||_W^2 = \int_0^1 F(r)\left(\frac{\theta^2}{r^2+\epsilon^2} + (\theta')^2\right)\mathrm{d}r \leq \left(\max_{0\leq r\leq 1} F(r)\right)\int_0^1 \left(\frac{\theta^2}{\epsilon^2} + (\theta')^2\right)\mathrm{d}r \leq A_1||\theta||_*^2 \tag{60}$$

where the Poincaré-inequality[8] was used in the last inequality, and

$$||\theta||_*^2 \leq \int_0^1 \left(\frac{\theta^2}{r^2+\epsilon^2} + (\theta')^2\right)\mathrm{d}r \leq \left(\min_{0\leq r\leq 1} F(r)\right)^{-1}\int_0^1 F(r)\left(\frac{\theta^2}{r^2+\epsilon^2} + (\theta')^2\right)\mathrm{d}r = A_2||\theta||_W^2, \tag{61}$$

which proves equivalence of both norms.
□

Of course, boundedness of $\{\zeta_i\}$, which has now been proven, is equivalent with boundedness of $\{\theta_i\}$. Now we know that in any reflexive space X, and thus in the Hilbert space W, the closure of any bounded set is weakly sequentially compact, i.e., any bounded sequence $\{x_i\}$ in W contains a subsequence that is weakly convergent to some limit $\bar{x}$. So in our case, $\{\theta_i\} \rightharpoonup \bar{\theta}$ for some $\bar{\theta} \in W$.
□

Question 4.2 *What properties does this weak limit have? In particular, what is the behaviour of $\theta_\epsilon(0,t)$ as $t \to T$, the maximal time of existence of θ_ϵ?*

Note that the same argument (in Lemma 4.5) cannot be used in the case where we have an energy-integral with an integrating factor r instead of $F(r)$ (as is the case when $\epsilon = 0$), for there we cannot establish equivalence of the norms $||\cdot||_*$ and $||\cdot||_W$.

So in the case where we prefix the boundary value $\theta(0) = \alpha$, there exists a solution to equation (51) for every value of the right boundary value Θ. We shall see in the next section that it is possible to say something about the behaviour of θ_ϵ in a heuristic way.

[8]We use the fact that the Poincaré-inequality for functions $u \in W_0^{1,2}(I)$, where I is a bounded and open interval in $\mathbb{R}$, can be applied as well for u that are zero on only one of the boundaries.

4.4 The semi-discrete problem in the case $\epsilon \neq 0$

Now we shall turn to the semi-discrete problem for $\epsilon \neq 0$. Let us try to repeat the argument used when $\epsilon = 0$. We will now have to consider the energy-integral

$$\mathcal{E}_{\theta_{\epsilon,i}}(\theta) = \int_0^1 \left(\frac{(\theta - \theta_{\epsilon,i})^2}{h} + \theta_r^2 + \frac{n^2 \sin^2 \theta}{r^2 + \epsilon^2} \right) F(r)\, \mathrm{d}r. \tag{62}$$

Note that we use a constant timestep h, to be fixed later. When this integral is minimized over the set $\{\theta \in W : \theta(1) = \Theta\}$ the solution $\theta_{\epsilon,i+1}$ to the following semi-discrete problem, corresponding to (40), is approximated:

$$\frac{\theta - \theta_{\epsilon,i}}{h} = \Lambda_\epsilon(\theta) \tag{63}$$

The notation and conditions are the same as in the case $\epsilon = 0$, equation (53).

Theorem 4.6 *For $h < h_0$, with h_0 sufficiently small and independent of $\theta_{\epsilon,i}$, there exists a unique minimizer $\theta_{\epsilon,i+1}(r)$ to (62) (so a unique minimizing solution to (63))*

Proof: The idea of the proof is the same as for $\epsilon = 0$. Because the functional $\mathcal{E}_{\theta_{\epsilon,i}}(\theta)$ is bounded from below (for instance by zero), there exists a minimizing sequence $\{\theta_j\}$ for this functional. We can show that this sequence has a minimizer in W by the same argument used in the proof of Proposition 4.4: the sequence $\{\theta_j\}$ is bounded, because the sequence $\{\theta_j - \Theta\}$ is bounded with respect to the norm $||\cdot||_*$ equivalent to $||\cdot||_W$. So there is weak convergence to a limit $\bar{\theta} \in W$.

Now for suitable time-stepsize h, there is a unique minimizer: Let u and v be two different minimizers. Then we have, because they both solve (63):

$$\frac{u - v}{h} = \Delta\,(u - v) - n^2 \frac{\sin 2u - \sin 2v}{2(r^2 + \epsilon^2)}$$

Let us call $(u - v) = f$. After multiplying by rf and integrating over $r \in (0, 1)$, we get:

$$\frac{1}{h} \int_0^1 r f^2 \,\mathrm{d}r = \int_0^1 r f \Delta f \,\mathrm{d}r - n^2 \int_0^1 r f \frac{\sin 2u - \sin 2v}{2(r^2 + \epsilon^2)} \,\mathrm{d}r \tag{64}$$

The right hand side is now smaller than the left side, when $\frac{1}{h} > \frac{n^2}{\epsilon^2}$: for then,

$$\left| -n^2 \int_0^1 r f \frac{\sin 2u - \sin 2v}{2(r^2 + \epsilon^2)} \,\mathrm{d}r \right| \leq n^2 \int_0^1 r|f| \frac{|f|}{(r^2 + \epsilon^2)} \,\mathrm{d}r \leq \frac{1}{h} \int_0^1 r f^2 \,\mathrm{d}r.$$

So for $h < \frac{\epsilon^2}{n^2}$ we have a contradiction, which proves that $u = v$.
□

Now that we have defined a sequence $\{\theta_{\epsilon,i}\}$ in this way, we again have the inequalities:

Proposition 4.7 *The sequence $\{\theta_{\epsilon,i}\}$, constructed by the above algorithm (63), (62), satisfies the following estimates on the energies:*

$$\mathcal{E}_{\theta_{\epsilon,i-1}}(\theta_\epsilon, i) \leq \mathcal{E}_\epsilon(\theta_{\epsilon,i-1}) \leq \mathcal{E}_{\theta_{\epsilon,i-2}}(\theta_{\epsilon,i-1}) \leq \mathcal{E}_\epsilon(\theta_{\epsilon,i-2}). \tag{65}$$

The proof runs in the same way as the proof of (56). There will also be a limit $\bar{\theta}_\epsilon$ for the sequence $\{\theta_{\epsilon,i}\}$. This $\bar{\theta}_\epsilon$, when extended to $[-1,1]$, will be a solution of (51). However, we cannot derive by this argument the value $\bar{\theta}_\epsilon(0)$ of this limit, for there exists a solution $\bar{\theta}_\epsilon$ to (51) for all left boundary values $\bar{\theta}_\epsilon(0) = \alpha$.

But we can still show in a heuristic way what values $\bar{\theta}_\epsilon(0)$ can take on. We will consider the following situation:

Example 4.3

Let $\theta_{\epsilon,k}$ be an element of the series $\{\theta_{\epsilon,i}\}$ and let

$$\delta = \inf\{r \in [0,1] \text{ s.t. } \theta_{\epsilon,k}(r) \geq \pi\}. \tag{66}$$

We will now compare the energies

$$\mathcal{E}_{\theta_{\epsilon,k}}(\hat{\theta}_{\epsilon,k}) \text{ and } \mathcal{E}_{\theta_{\epsilon,k}}(\bar{\theta}),$$

where both functions are defined as modifications of $\theta_{\epsilon,k}$ as follows:

$$\hat{\theta}_{\epsilon,k} = \bar{\theta} = \theta_{\epsilon,k} \qquad \text{for} \qquad r \in (\delta, 1);$$
$$\hat{\theta}_{\epsilon,k} = \eta + \frac{\pi - \eta}{\delta} r \qquad \text{for} \qquad r \in (0, \delta) \qquad \text{and}$$
$$\bar{\theta} = \pi \qquad \text{for} \qquad r \in (0, \delta).$$

Here $\eta = \hat{\theta}_{\epsilon,k}(0)$ can be any number in $(0, \pi)$, but the most interesting case arises when η is small. The question is, which of $\hat{\theta}_{\epsilon,k}$ and $\bar{\theta}$ is a better minimizer of $\mathcal{E}_{\theta_{\epsilon,k}}$? We will show that when δ becomes sufficiently close to zero,

$$\mathcal{E}_{\theta_{\epsilon,k}}(\hat{\theta}_{\epsilon,k}) > \mathcal{E}_{\theta_{\epsilon,k}}(\bar{\theta}). \tag{67}$$

From this we infer that $\bar{\theta}$ (i.e. a function that has "jumped" in $r = 0$) is a better candidate to be a minimizer[9] of (62) than $\theta_{\epsilon,k}$. By simplifying (67), we see that is satisfied when

$$\int_0^\delta F(r) \frac{(\bar{\theta} - \hat{\theta}_{\epsilon,k})^2}{h} \, \mathrm{d}r < \int_0^\delta F(r) \left((\hat{\theta}_{\epsilon,k})_r^2 + \frac{n^2 \sin^2 \hat{\theta}_{\epsilon,k}}{r^2 + \epsilon^2} \right) \mathrm{d}r, \tag{68}$$

[9]Notice the tacit assumption that $\theta_{\epsilon,k}$ behaves as a linear function as $r \to 0$. This is not justified, but we believe that in principle this assumption may be removed by considering nonlinear $\hat{\theta}_{\epsilon,k}$ on $(0, \delta)$. Although we did not prove this, we assert that there would still be a positive δ such that $\bar{\theta}$ would be a better minimizer than $\theta_{\epsilon,k}$ itself. The calculations would be much more difficult in this case; we omitted them for simplicity.

because the other terms in the integrals drop out. We estimate both integrals. The reader can do the computations by himself (and may be he can improve these estimates):

$$\int_0^\delta F(r)\frac{(\bar{\theta}-\hat{\theta}_{\epsilon,k})^2}{h}\,\mathrm{d}r < \frac{\delta F(\delta)}{3h}(\eta-\pi)^2;$$

$$\int_0^\delta F(r)\left((\hat{\theta}_{\epsilon,k})_r^2+\frac{n^2\sin^2\hat{\theta}_{\epsilon,k}}{r^2+\epsilon^2}\right)\mathrm{d}r > F(0)\left(\frac{(\eta-\pi)^2}{\delta}+\frac{\delta(\pi-\eta+\frac{1}{2}\sin 2\eta)}{2(\delta^2+\epsilon^2)(\pi-\eta)}\right),$$

so that if

$$\frac{\delta F(\delta)}{3h}(\eta-\pi)^2 < F(0)\left(\frac{(\eta-\pi)^2}{\delta}+\frac{\delta(\pi-\eta+\frac{1}{2}\sin 2\eta)}{2(\delta^2+\epsilon^2)(\pi-\eta)}\right),$$

(68) will be satisfied. This is (again after many simplifications) certainly the case for

$$\delta \le (3hF(0))^{\frac{1}{3}}.$$

This is only a very rough estimate, but it shows us that the time stepsize h plays an important role: the smaller h is, the less easy it will be to make large jumps. Also, $F(0)=\sqrt{1+\epsilon^2}-1$, so for small ϵ the conditions on jumping are more strict than for large ϵ.

We do not know whether (and under what conditions) δ decreases fast enough as $k\to\infty$, in order to force $\theta_{\epsilon,i}(0)$ to jump. We conjecture, however, that this happens in many cases. This is also confirmed by the numerical results in the next chapter.

In sum: this example shows us, that problem (40)-(42) is not very suitable for predicting blow-up of the exact solution to (10)-(13).
□

We conclude by summarizing: the study of the semi-discrete problems has learned us, that numerical approximations that are very accurate (or even exact, in this case) in the spatial variable may blow up numerically (in whatever sense) under conditions different from the FTB-conditions for the exact solution to (10)-(13).

5 Interpretation of the output of the Zegeling code

In this chapter, the output of the Zegeling code will be presented and interpreted, bearing in mind the conclusions of the previous chapter.

5.1 Preliminaries

This information will be relevant when the reader examines the figures and graphs that this chapter contains:
The following parameters and features of the code can be varied:

- n,
- ϵ,
- $NPTS$, the number of spatial grid points (odd because of symmetry considerations),
- TF, the final time of the computation,
- the initial and boundary conditions, induced by θ_0,
- the use of a fixed grid or of a moving grid.

It is possible to change the domain on which the approximations are made from $[-1, 1]$ to $[-R, R]$. To do this, some adaptations will need to be made in the code; see section 5.7 below on this. For further details on the code itself, the reader is referred to [10].

Unless stated otherwise, all data examined have been obtained from the following initial-boundary conditions on problem (40):

$$\theta_0(r) = 2.25\pi r^2, \qquad \theta(\pm 1, t) = 2.25\pi \tag{69}$$

The code gives output in a data file. We wrote a file in MATLAB to present the output of the code graphically. The definition that follows will fix the notation of the numerical approximations:

Definition 5.1 *We shall call a numerical solution at gridpoint* (x_m, τ_l)

$$u_m^l = u(x_m, \tau_l),$$

where the index $m \in \mathbb{Z}$ *for the spatial variable ranges from* $M^- = -\frac{NPTS-1}{2}$ *to* $M^+ = +\frac{NPTS-1}{2}$ *and the index* $l \in \mathbb{N}$ *of the temporal variable ranges from* 0 *to* 100*, where* $\tau_l = \frac{l}{100}TF$*. Remark that we write (by slight abuse of notation)* x_m *shorthand for* $x_m(\tau_l)$ *(the spatial grid is different at each* τ_l*)*[10].
We shall write $u_m^l(n, u^0, ...)$ *to denote the dependence of the approximation on the parameters* n*,* u_0*, etc. mentioned above.*

So an approximation u^l is computed at each one-hundredth of the final time TF, with the solution given in pairs $(x_m, u^l(x_m))$ for all m. Each figure shows the approximation u_m^L for all x_m at a time τ_L. Here L is either a multiple of 10, or L can be the last

[10]It is not the case that the grid is changed only at a discrete number of time points. On the contrary, the spatial grid is moved continuously in the space-time domain. But of course, the code can only present its output at a discrete number of time points.

registered timestep *before* or the first registered timestep *after* the numerical blow-up. (Recall our definition 3.1 of numerical blow-up.) The pairs (x_m, u_m^l) are indicated in the figures by stars.

Finally, we remark that the approximation u_m^l is compared both with the solution θ to (10)-(13) and with the solution θ_ϵ to (40)-(42). When we use θ and θ_ϵ without further specification, they will always denote such solutions.

5.2 When does the approximation u_m^l blow up?

In the previous section we saw that a lot of parameters can be varied when running the code. In the present section, we will vary some of them and see what their influence is on the numerical approximations.

Example 5.1 *(See figure 2)*

A typical example of an approximation to problem (40) with numerical blow-up according to definition 3.1 is shown in figure (2) (zoomed in on the blown up part of the figure).

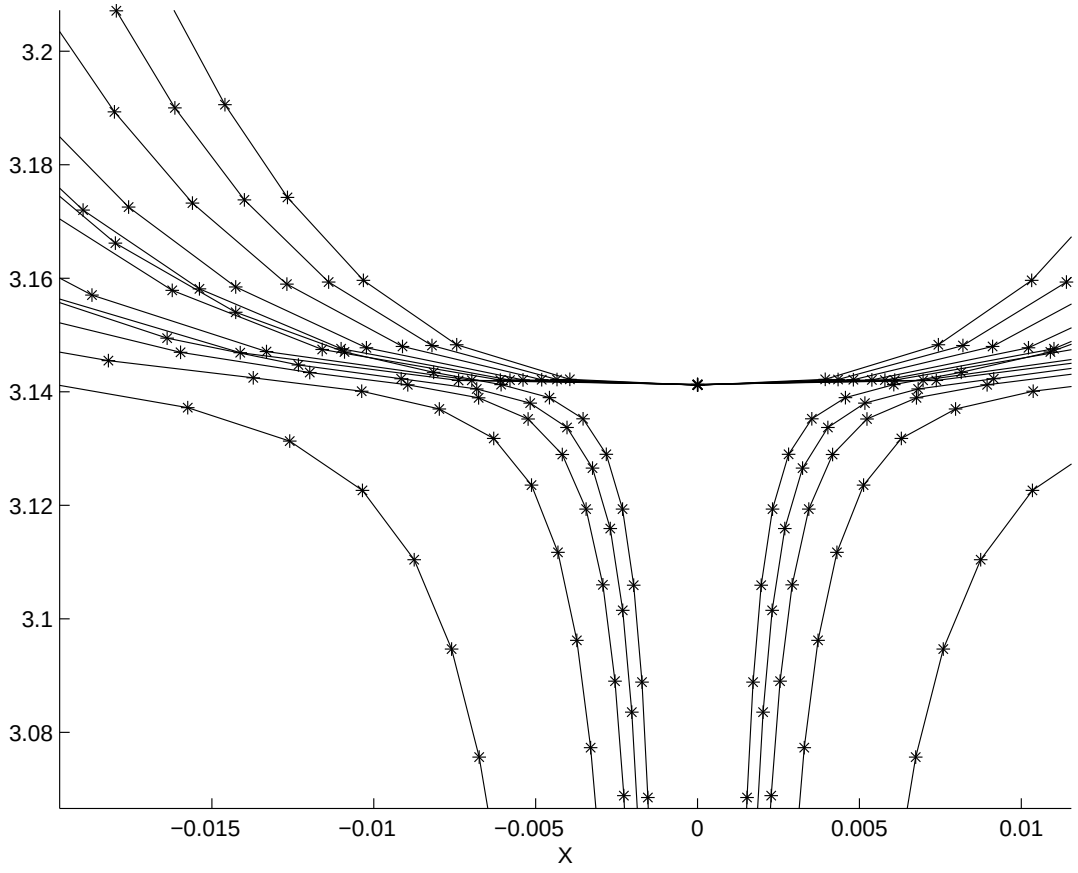

Figure 2: Behaviour of the numerical blow-up of the moving grid approximation: an example ($\epsilon = 10^{-6}$, $NPTS = 101$ and $n^2 = 5$)).

In the figures there are no indications to which time τ_l a certain graph corresponds. But it is easy to see that, the lower a graph is plotted, the smaller the time τ_l is that it corresponds to. In other words, the larger the discrete derivative of u_m^l near $r = 0$ is, the larger τ_l.

In a way analogous to definition 2.1, we can try to define numerical blow-up as follows for moving grid approximations:

We say that an approximation u_m^l to problem (40)-(42), obtained by a moving grid scheme, blows up numerically if the first grid point x_1^l decreases 'fast enough' as the time τ_l increases.

The rationale for this attempt of a definition is the following: In terms of the moving grid scheme, the growth of the discrete derivative of u_m^l near $r = 0$ is equivalent with the grid becoming more refined near $r = 0$. But it is not so clear how we should specify 'fast enough'. If this defintion is to work, we will have to consider approximations u_m^l for many different parameters to justify its use empirically.

Remarkable about this example is, that in the exact solution to (10)-(13), there is no finite time blow-up for this value ($n^2 = 5$) of n. But for most choices of the parameter n and of the initial condition u_m^0, the numerical approximation showed the blow-up behaviour that was expected from the analysis of the exact problem (10)-(13).

But there is a problem here: was the "correct" numerical blow-up behaviour for this particular value of n and this initial condition seen for many different choices of the other parameters (ϵ, $NPTS$, TF, etc), or only for some choices? This problem arises for any definition of numerical blow-up that we choose in terms of the solution $u_m^l(n, u^0, \epsilon, NPTS)$ for a certain fixed set of parameters.

For instance, if $\epsilon = 10^{-9}$ (and the same values of the other parameters in figure 2) there is no numerical blow-up anymore. *Is* there something like a correct numerical blow-up behaviour, given a choice of n? In order to answer the question, whether θ blows up in finite time for a given value of n (i.e. our Main Question 1.1), we will try to answer the following question:

Question 5.2 *For which relation of the parameters ϵ and $NPTS$ does the numerical approximation $u_m^l(n, u_m^0)$ show blow-up behaviour that matches with the blow-up behaviour of θ?*

It is logical to consider $\epsilon \to 0$, $NPTS \to \infty$: one expects that the blow-up behaviour of u_m^l corresponds better to that of θ as we approach this limit. But as we shall see in section 5.6, things are not that simple. Question 5.2 is an empirical question to the extent that we can compare the behaviour of the approximations $u_m^l(n, u_m^0)$ for various parameter values with that of the exact solution θ; but it is an analytical question insofar as we can analyse the rate of convergence of δ (the parameter defined in (66)) to zero and show in which cases, in general, we can expect numerical blow-up.

For the time being, we shall assume that u_m^l is an (in some sense) accurate approximation to the solution θ_ϵ of (40), if $NPTS$ is large enough. We shall also assume,

that θ_ϵ behaves in a way that is reflected in the approximation by numerical blow-up. This is justified in part, because both the numerical approximation u_m^l and the semi-discrete problem (63) blow up numerically under certain conditions. But as we saw in Example 4.3, it is by no means clear that θ, the solution to (10), will have the same blow-up behaviour as θ_ϵ. And it is about the blow-up behaviour of θ that we want to draw a conclusion.

5.3 The initial condition; the difference between moving and fixed grid schemes

We will now focus on the numerical scheme itself and examine the following question:

Question 5.3 *Can and does the choice of different initial conditions u_m^0 influence the numerical blow-up behaviour of u_m^l?*

I use the same initial conditions as given in (69) throughout this paper, unless the contrary is indicated. The purpose of the choice $u_{M^\pm}^l > 2\pi$ is to allow u_m^l to jump once or twice when the corresponding exact solution $\theta(r,t)$ does so. The initial condition u_m^0 is a quadratic function. It was not chosen to be linear, because the approximations to (40) are symmetric. But other u_m^0 could have been chosen that are also symmetric around $r = 0$.

To obtain the following pictures 3 and 4, we took the initial value $u_0^0 = 1$ such that $|u_0^0 - k\pi|$ is large for all k. These pictures suggest that it is reasonable to consider initial conditions satisfying $u_0^0 = 0$ only: we see that, when we use a moving grid, as in figure 3, u_0^l immediately tends to the multiple of π that is (in some way) "nearest" to $u_0^0 = 1$. In our case this value is $u_0^0 = 0$ (but if the discrete derivatives near $r = 0$ of u_m^0 are suitably large, this value will be $u_0^0 = \pi$). Figure 4, obtained using a fixed grid, is included for comparison. Also for comparison, we include in figures 5 and 6 (for the same values of the other parameters) the approximations for our default initial conditions.

Answer to Question 5.3: We infer from pictures 3-6, that different initial conditions give rise (*ceteris paribus*) to approximations with the same numerical blow-up behaviour.

Considering the figures with regard to the influence of the initial conditions, it seems that there is a huge difference between moving grid and fixed grid approximations:

Question 5.4 *Is it necessary to use a moving grid scheme in order to approximate the solution to (40) accurately? Do fixed grid solutions also show numerical blow-up?*

Figures 3 and 4 suggest that the moving grid approximation can blow up, but that approximations obtained by the fixed grid method show strange behaviour around

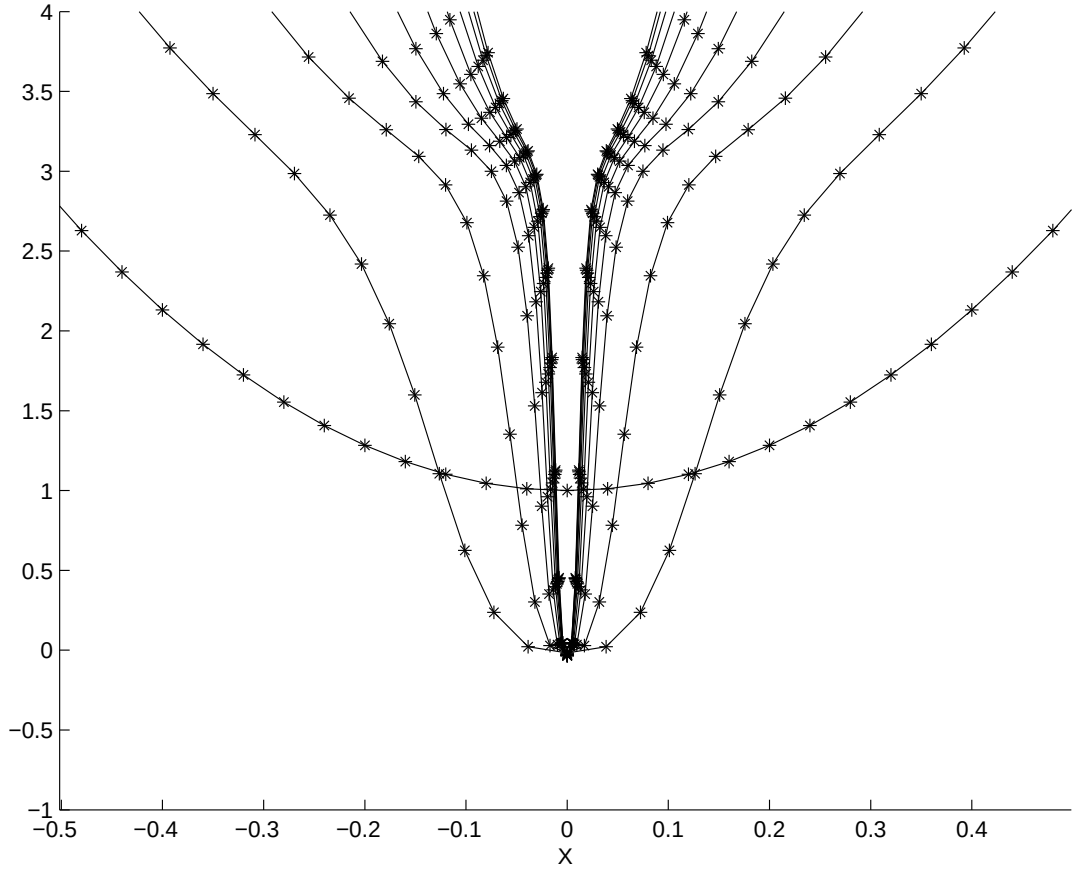

Figure 3: Enlarged picture of the solution to (40) where a moving grid has been used, with initial function $u^0(r) = 1 + 2.25\pi r^2$. Parameters $\epsilon = 10^{-8}, n^2 = 8, TF = 1, NPTS = 51$

$r = 0$. This difference in blow-up behaviour could be due to the fact, that there are too few gridpoints around $r = 0$ on the fixed grid. For the exact solution θ (or θ_ϵ), this is the region that contributes most to the integral $\mathcal{E}$ or $\mathcal{E}_\epsilon$ respectively. (We shall say more about the energy in section 5.4.)
Indeed, when we enlarge $NPTS$ given a certain ϵ for the fixed grid, the approximation behaves better, but not very well yet, for the solution at $r = 0$ still deviates from zero (see figure 7). Only for extremely large $NPTS$ (and, as we shall see in section 5.6, only for a certain relation between ϵ and $NPTS$) the fixed grid approximation behaves more like the moving grid approximation: $|u_0 - 0|$ is large only when this is true as well in the moving grid case, and there is numerical blow-up in some cases. This last fact is shown in figures (8) and (9).

Another remark to be made here is that for very small ϵ (this value turns out to be about 10^{-12} for $n = 1$), the moving grid scheme gets stuck in the computations. According to Zegeling, this is probably due to the code and not to the computing capacity of the machines we used. The fixed grid can compute approximations up

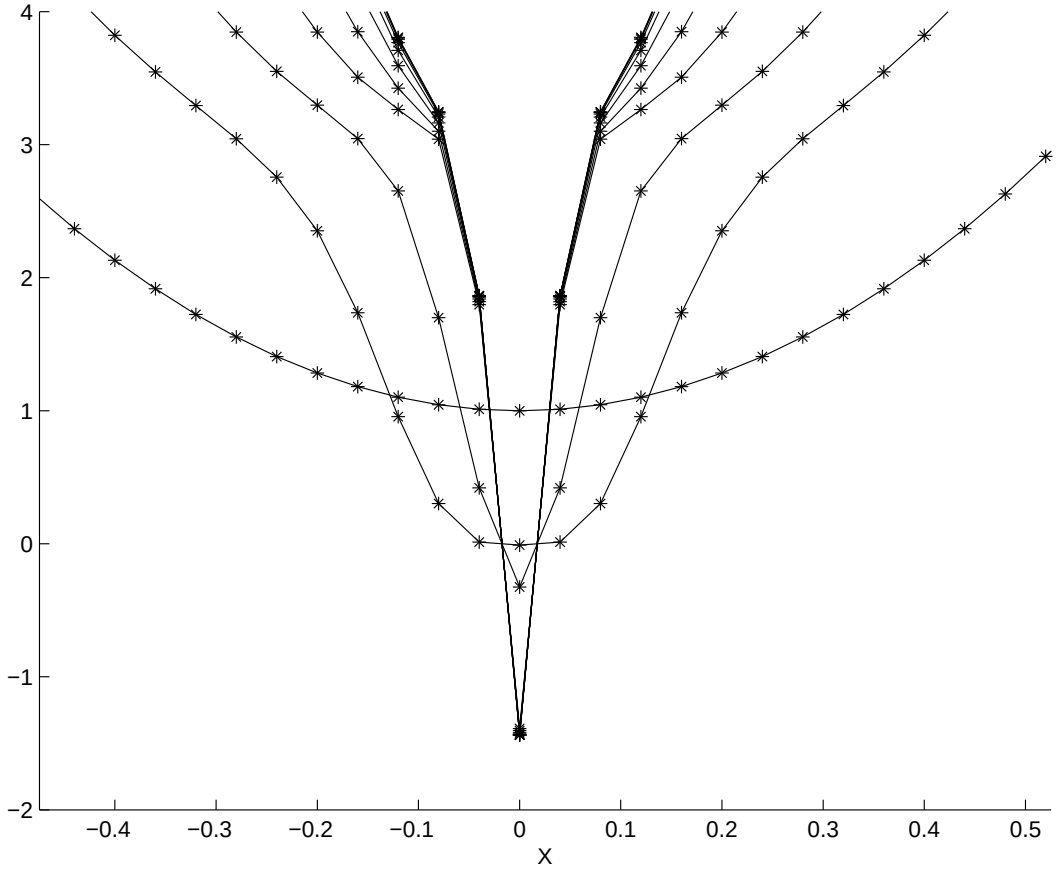

Figure 4: Enlarged picture of the approximation to (40)-(42) with initial condition $u^0(r) = 1 + 2.25\pi r^2$, where a fixed grid has been used. The difference with figure 3 clearly shows the advantage of the moving grid: here, the fixed-grid approximation tends towards some clearly negative value for $r = 0$. The other conditions are the same as in figure 3

to $\epsilon = 10^{-15}$. But for these values of ϵ, very large values of $NPTS$ are needed to make sense of the fixed grid approximations, and again the program gets stuck in the computations.

Answer to Question 5.4: It is possible to obtain approximations $(u_m^l)_{Fix}$ for the fixed grid, for large ϵ, that behave as accurate as the corresponding moving grid approximation $(u_m^l)_{Mov}$. But to obtain sensible approximations for smaller ϵ, it is necessary to choose $NPTS$ very large, in fact so large that the computing times are too large. For our purposes it makes sense to study moving grid approximations only.

Now that we have motivated the choice for considering moving grid solutions for initial u^0 as in (69), we will sketch the content of the remaining sections of this final chapter. As we saw (for example in Question 5.4), it turns out that the occurrence of numerical blow-up depends, among others, on the relation bewteen ϵ and $NPTS$.

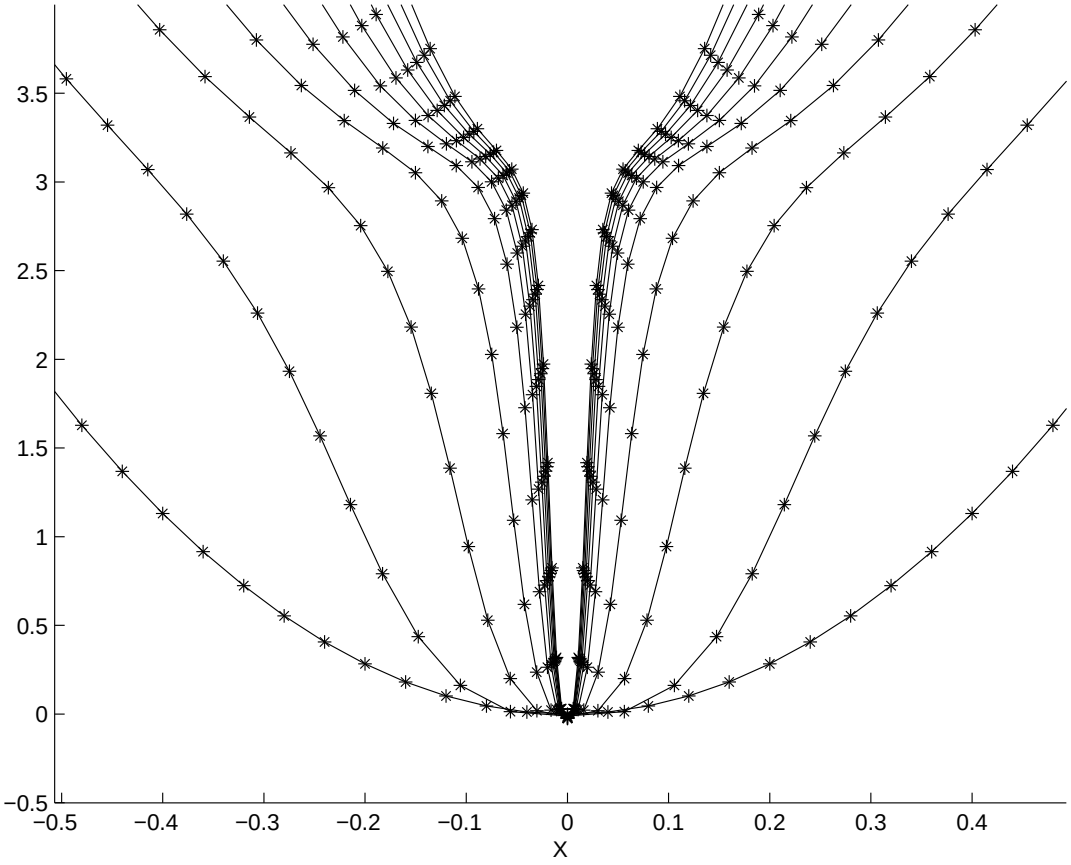

Figure 5: Enlarged picture of the moving grid approximation to (40), with initial function $u^0(r) = 2.25\pi r^2$. Parameters as in figure 3

We will examine this dependence in section 5.6 for two values of n.

A final problem that we will mention is the choice of the final time of the algorithm, TF: in principle, the FTB in problem (10) may occur for any $T \in \mathbb{R}$, while computations may take too long for very large TF that we choose in the approximation. For this question, which is only briefly mentioned in this paper, see section 5.7.

However, first we will consider the discrete energy (a numerical equivalent of the energy $\mathcal{E}_\epsilon$) in the next two sections. It has been explained in chapter 2, that the exact value $\theta(0,t)$ is a multiple of π for $t > T$. But why can (in the numerical approximation) $|u_0^l - k\pi|$ sometimes be so large for $\tau_l > BUT$? In the next section, we shall introduce our method of measuring the discrete energy ($DE(u_m^l)$). After that, we shall try to explain the fact that $|u_0 - k\pi|$ is quite large for so many different parameter values.

5.4 Measurement of the energy of the numerical solution

We have computed, for each numerical approximation $u_m^l\,(l = 0, 1, ..., TF\,, m = M^-, ..., 0, 1, ..., M^+)$ to problem (40), an approximation of the energy correspond-

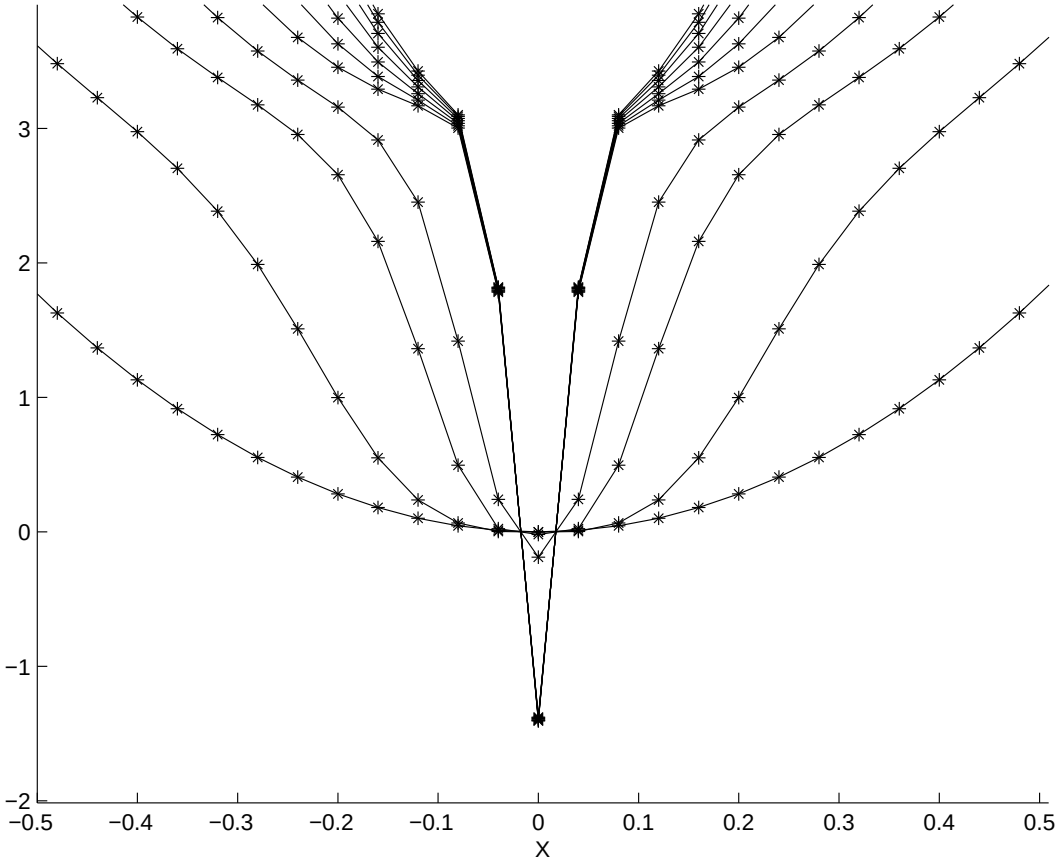

Figure 6: Enlarged picture of the fixed grid approximation to (40), with initial function $u^0(r) = 2.25\pi r^2$. Parameters as in figure 3

ing to u_m^l at various time points τ_l. The numerical scheme by which this was done for each τ_l is the following: We compute the energy-approximation only for positive values of r. That is, we compute the approximation to $\frac{1}{2}\mathcal{E}_\epsilon$, as defined in (50). The number of gridpoints M in the spatial variable, with respect to which we integrate, is determined by the number of gridpoints $NPTS$ used in the Zegeling code. Thus we get the sum (where we have left out the superscript l's indicating the time τ_l at which the computation is done):

$$DE = \frac{1}{2}\left\{\sum_{i=1}^{M-1}\left(G^+(x_i) + G^-(x_i)\right) + G(x_0) + G(x_M)\right\}, \tag{70}$$

where

$$G^+(x_i) = \frac{x_i + \sqrt{x_i^2+\epsilon^2}}{1+\sqrt{1+\epsilon^2}}\,(x_{i+1}-x_i)\left\{\frac{1}{4}\left(\frac{u_{i+1}-u_i}{x_{i+1}-x_i} + \frac{u_i - u_{i-1}}{x_i - x_{i-1}}\right)^2 + \frac{n^2\sin^2 u_i}{x_i^2+\epsilon^2}\right\}, \tag{71}$$

with

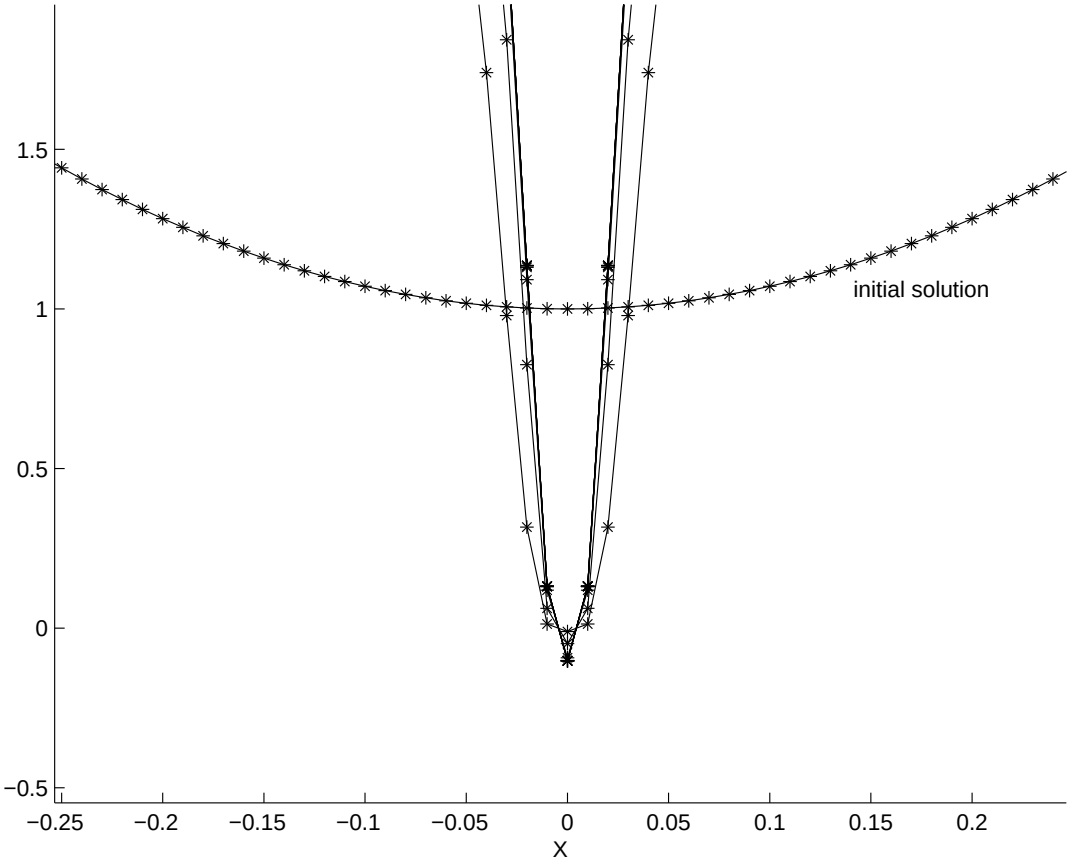

Figure 7: Close-up of the fixed-grid solution to (40), under the same conditions as in figure 4 save that $NPTS = 201$ here. The fixed grid behaves better, for $\theta(0, t_i) \approx -0.1$ is not very far from zero, but not good enough considered that $NPTS$ is large and that $\epsilon = 10^{-8}$.

$$G(x_0) = \frac{\epsilon^2}{1 + \sqrt{1 + \epsilon^2}} \frac{x_1}{2} \frac{n^2 \sin^2 u_0}{\epsilon^2}, \tag{72}$$

and where

$$G^-(x_i) = \frac{x_i + \sqrt{x_i^2 + \epsilon^2}}{1 + \sqrt{1 + \epsilon^2}} (x_i - x_{i-1}) \left\{ \frac{1}{4} \left(\frac{u_{i+1} - u_i}{x_{i+1} - x_i} + \frac{u_i - u_{i-1}}{x_i - x_{i-1}} \right)^2 + \frac{n^2 \sin^2 u_i}{x_i^2 + \epsilon^2} \right\}, \tag{73}$$

with

$$G(x_M) = \frac{x_M + \sqrt{x_M^2 + \epsilon^2}}{1 + \sqrt{1 + \epsilon^2}} (x_M - x_{M-1}) \left\{ \left(\frac{u_M - u_{M-1}}{x_M - x_{M-1}} \right)^2 + \frac{n^2 \sin^2 u_M}{x_M^2 + \epsilon^2} \right\}. \tag{74}$$

This way of approximating will be called $DE(u_m)$ or *discrete energy*. We are dealing here with an approximation of the integral of the numerical approximation to (40).

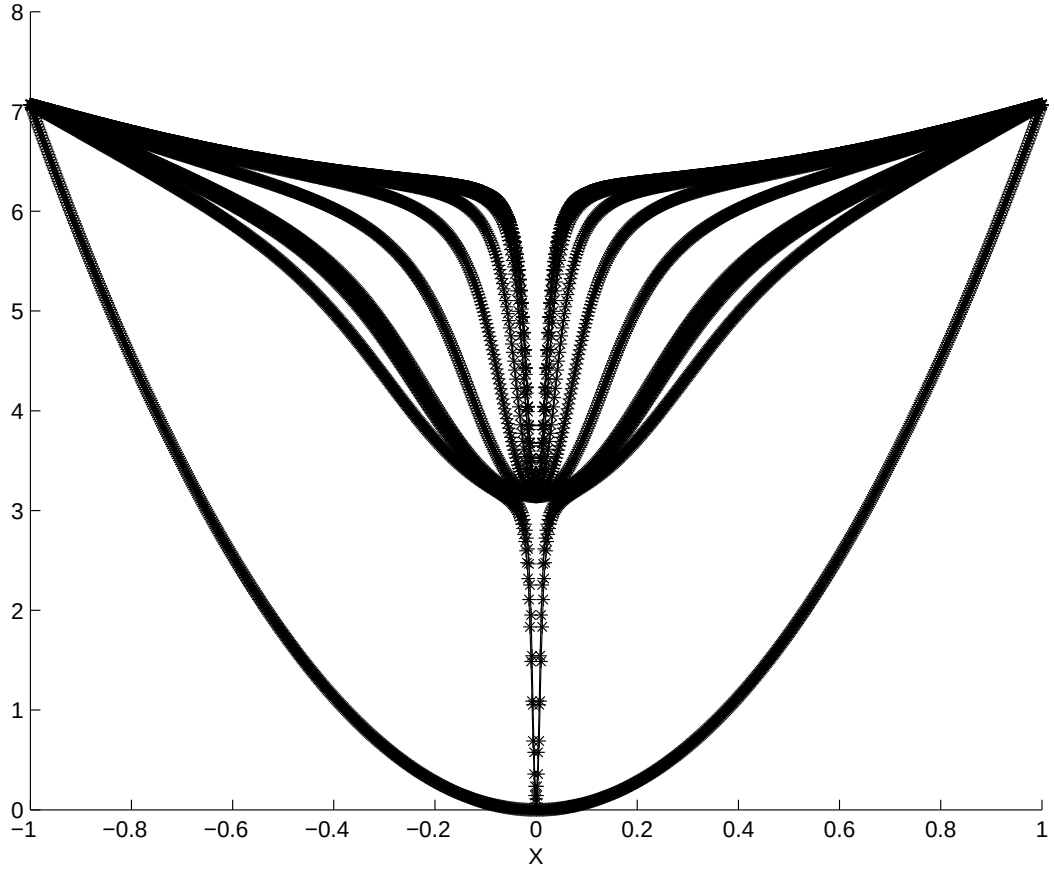

Figure 8: Fixed-grid solution to (40), where $NPTS = 1001$ is very large. The other parameters are $\epsilon = 10^{-5}$, $n = 2$, $TF = 3$. The fixed grid solution shows numerical blow-up for these parameter values. Compare this to figure 9, where there is not one jump, but two jumps (under the same conditions).

Note that the computation of the discrete energy can only be refined by taking more gridpoints in the computation of u_m; so we cannot refine *the* approximation of the energy corresponding to a given numerical solution u_m.

Question 5.5 *Is the above method of approximating the energy $\mathcal{E}_\epsilon$ for numerical approximations u_m^l accurate (in some sense)?*

A weak point of the above method of numerical integration might be, that it uses a centered difference approximation for the derivatives of θ, while the Zegeling code probably uses a more sophisticated way of approximation. However, there was no time do investigate the code deeply in this respect and, as we shall see in the next question, the method of integration described above does well for our purpose, which is to establish an energy principle analogous to the exact principle (52)[11]

[11]It is inconceivable in our view (although we did not analyse the numerics) that the DE is nonincreasing in time *because of* the wrong method of integration used. We believe that the DE is nonincreasing in time *in spite of* this possibly poor method of approximation.

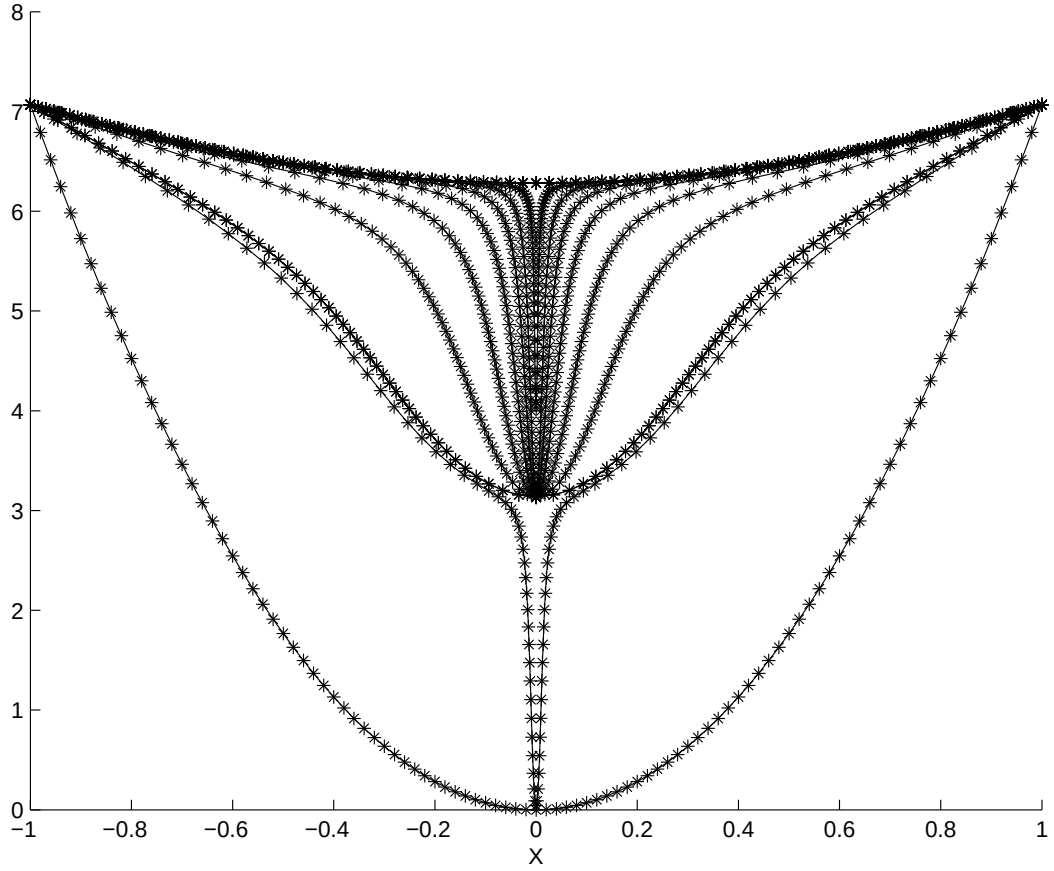

Figure 9: Moving-grid solution to (40), where $NPTS = 101$. The other parameters are the same as in figure 8, to which this plot should be compared. The moving grid solution shows numerical blow-up twice here for $NPTS$ much smaller than the fixed grid solution, which blows up only once.

The energy $\mathcal{E}_\epsilon(\theta_\epsilon)$ is never increasing in time, as we saw in (52). Now we ask:

Question 5.6 *Does $DE(u_m^l)$ ever increase in time?*

We expect that the numerical approximation E_ϵ to $\mathcal{E}_\epsilon$, given by replacing u_i with $\theta_\epsilon(x_i)$ in (70), does not increase either. But, as we remarked above, we deal in this section with the discrete energy DE, an approximation of the energy corresponding to u_m^l, which is itself an approximation of the solution θ_ϵ to (40). This approximation u_m^l prescribes the gridpoints at which we integrate the energy numerically.

Answer to Question 5.6: It turns out, that the sequence of discrete energies, $\{DE(u_m^l)\}_{l=0}^{100}$ corresponding to *moving-grid* approximations never increases with the time τ_l.

For a *fixed grid*, however, the behaviour of the discrete energy depends upon choices of $NPTS$ and ϵ. We saw already in figure 6 that the fixed grid solution does not behave like θ_ϵ very much. In most cases, the DE is not monotonely decreasing.

But, to take the example of figure 8, when $\epsilon = 10^{-5}$ and $NPTS = 1001$, there is numerical blow-up and the DE is non-increasing.

In general, the increasing of the discrete energy takes place in approximations that looked inaccurate. This confirms our answer to Question 5.5, that the way of defining DE is not too bad.

The DE does not only decrease monotonically, we also see a big jump in DE when there is blow-up: if numerical blow-up occurs between times l_k and l_{k+1},

$$DE(u_m^{l_{k+1}}) - DE(u_m^{l_k}) << 0.$$

□

5.5 Continuous blow-up and energy considerations

A phenomenon worthy of attention is *continuous blow-up* or CBU, as is shown in figure 10, which contains a close-up to the approximation in figure 9. Characteristic of what we call CBU is, that the numerical blow-up takes place in more than one timestep. This phenomenon might have something to do with the behaviour of the discrete energy.

In figures 9 and 10 we chose the parameters $\epsilon = 10^{-5}$, $NPTS = 101$, $n = 2$. When ϵ is quite large, like in the case of these figures, there is no numerical blow-up according to definition 3.1, where we have to choose η close to zero. But there still is a kind of blow-up, as the approximation u_0^l tends from 0 to π in a small number of timesteps: two in the case of figure 10, but often more. The fact that this increase in u_0 happens in an *apparently* continuous manner is the reason for the name CBU.

Question 5.7 *For which numerical approximations u_m^l does CBU occur, and why?*

Answer: If ϵ is decreased in the situation of figures 9 and 10, the CBU will disappear. For other parameter values, CBU is only seen for large ϵ as well. One could be tempted to ascribe the occurrence of CBU to bad energy behaviour of the code: one expects that it is not possible to have, at a time τ_l, $|u_0^l - k\pi|$ far away from zero for all k without having an increase in DE. However, we saw in the previous section that the DE correpsonding to moving grid approximations never increases. Moreover, we saw in example 4.3, in the semi-discrete problem for $\epsilon \neq 0$, that the values, that $\bar{\theta}_\epsilon$ may assume, do not form a discrete spectrum, like in the case $\epsilon = 0$. So the phenomenon of CBU is not a complete surprise.

The energy behaviour is peculiar at the timesteps where the CBU takes place. The DE typically stays approximately the same for a long time, but in the (one of few) timesteps where blow-up occurs (be it numerical or continuous blow-up), the DE suddenly decreases drastically. This suggests that CBU is an intermediate case between (a) u_m^l blowing up numerically and (b) u_0^l staying close to zero for all l, that

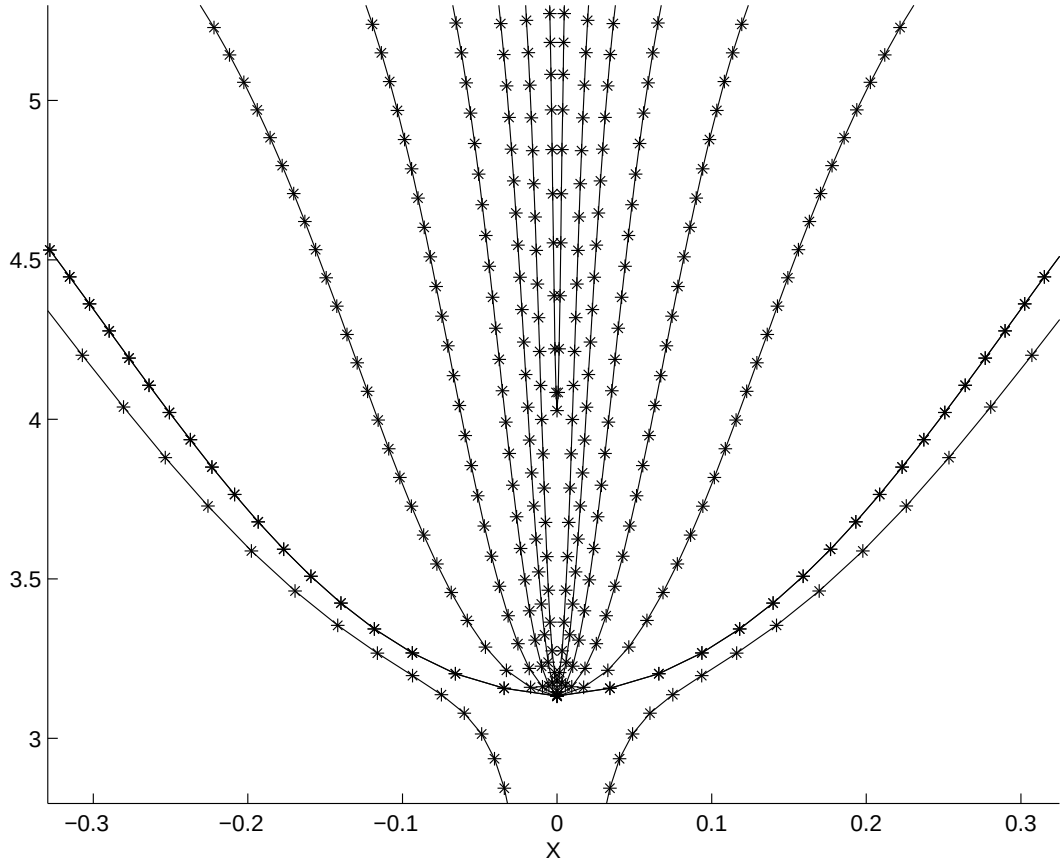

Figure 10: Close-up of the approximation shown in figure 9. $u_0^L \approx 4$, where L is the timestep before u_0 jumps to 2π. There is continuous blow-up for the approximation in this case, because the approximation takes more than one timestep to jump from $u_0 \approx \pi$ to $u_0 \approx 2\pi$.

is not principally different from those two other cases. In other words, we expect that in *both* cases (a) and (b), the corresponding exact solution $\theta_\epsilon(r,t)$ increases in a continuous way from 0 to π for $r = 0$ and $t \in (t_0, t_1)$.
□

Although we do not have a proof of why CBU occurs, we expect that it occurs for the same reason as "normal" numerical blow-up. In the next section, we shall conclude that the relation between x_i and ϵ is very important in explaining the numerical blow-up. This relation also explains why there is artificial blow-up (i.e. numerical blow-up of u_m^l in cases where θ, the solution to (10)-(13), does not blow up in finite time).

5.6 The relation between x_i and ϵ

We already encountered (in section 5.2, Question 5.2) a problem with the interpretation of the output. This problem was, when we could judge that a *set* of approximations, where n and u_m^0 were kept fixed, has numerical blow-up. Such a set corresponds to the solution θ of one particular instance of problem (10)-(13). Take the example $n = 3$, $TF = 3$ and the initial condition u_m^0 defined in (69). For a fixed number of space points $NPTS = 101$, if ϵ equals 10^{-3} there is numerical blow-up. But if we gradually decrease ϵ, the blow-up time becomes larger, and eventually the numerical blow-up disappears.

We could be very pleased with this result, as global existence is what we expect for the exact solution θ to (10)-(13) in the case that $n > 2$, and global existence of $u_m^l(n, u^0)$ seems to be implied by the results for decreasing ϵ. But existence for all time of u_m^l can never be proven by this numerical scheme. A possible interpretation of the disappearance of numerical blow-up is, that there is still numerical blow-up for small ϵ, but that the time of blow-up BUT is far beyond TF now. In section 5.7, a suggestion to deal with the numerical problem of too large computational times TF is described.

The table that follows now was made under the conditions $n = 3$, moving grid, $TF = 3$, $u_m^0 = 2.25\pi\sqrt{x_m}$. In all the tables that are to follow, the values (one or two) in the table grid indicate the numerical blow-up time, if there was numerical blow-up (with an X for "no numerical blow-up") that corresponds to the given values of ϵ and $NPTS$. Dots indicate that the approximation was not done for those particular values.

$NPTS$	41	101	201	401	1001
$\epsilon = 10^{-3}$	5	CBU	CBU	...	...
$\epsilon = 10^{-4}$	X	9	8	...	...
$\epsilon = 10^{-5}$	...	35	15	14	...
$\epsilon = 10^{-6}$	...	X	35	22	21
$\epsilon = 10^{-7}$	...	X	X	X	31

For $\epsilon = 10^{-8}$ the times of computation became very large here. One sees in this table, that also for very small ϵ, a value of $NPTS$ could be found for which there is numerical blow-up. For larger ϵ (10^{-2}, 10^{-1}) the approximation blows up immediately and also for very low $NPTS$.

The table that follows was made with $n = 1$, moving grid, $TF = 1$ or $TF = 3$ and regular u^0.

$NPTS:$	31	51	101	201
$\epsilon = 10^{-3}$	...	...	CBU, 39	CBU, 39
$\epsilon = 10^{-4}$	14, 51	14, 50	14, 49	14, 49
$\epsilon = 10^{-6}$	...	18, 67	17, 63	17, 63
$\epsilon = 10^{-7}$	18	21, 73	19, 69	18, 67

In the cases $\epsilon = 10^{-3}$ and $\epsilon = 10^{-4}$, there was CBU. From this table it is clear, that for $n = 1$ the blow-up behaviour of the approximation $u^l_m(n, u^0)$ does not depend very much on ϵ. When ϵ is large, there is CBU for the same reason as in the semi-discrete case. Even when $NPTS$ is small for such ϵ, there is no interference of the two parameters.

A table produced for $n = 4$, moving grid, $TF = 3$, regular u^0.

$NPTS:$	51	501
$\epsilon = 10^{-2}$	16	15
$\epsilon = 10^{-5}$	X	87
$\epsilon = 10^{-9}$	X	X

Although we see no numerical blow-up anymore in the case $\epsilon = 10^{-9}$, we expect that for larger $NPTS$ there will be numerical blow-up. But the times of computation became too large for larger $NPTS$. We remark that, although it does not contain as many results, this table resembles the table for $n = 3$.

So in the case $n = 3$, where analytically FTB cannot occur for any initial $\theta(r, 0)$, we expect that for increasingly smaller ϵ numerical blow-up is not seen anymore. But the data in the above tables suggest that we can expect numerical blow-up for $t < 3$ for any ϵ and for any n, if only we make $NPTS$ large enough. This is very strange, because one would expect a greater accuracy when $NPTS$ is increased.

We know that the code approximates not θ but θ_ϵ. But this does not explain the following yet: why would it hold that $\theta_\epsilon(0, t) \to \pi \pm \eta$ for small η, as $t \to T$? For the semi-discrete problem, we could explain *why* numerical blow-up would occur, but not *when* it would occur. However, we have a way to explain this seemingly inaccurate behaviour:

Question 5.8 *Why is there always numerical blow-up for u^l_m when $NPTS$ is made large enough (for fixed values of the other parameters)?*

We saw in section 5.4, that the discrete energy $DE(u^l_m)$ corresponding to the moving

grid approximations was non-increasing in all the cases considered. We shall therefore *assume* now that this energy principle,

$$DE(u_m^l) < DE(u_m^{l-1}),$$

for all $l > 0$, holds for all moving-grid approximations that we considered.

We saw as well, as time approaches TF, that the space points x_i in the approximation become more numerous in the interval $(0, \delta)$. This happens for all values of the different parameters, and most notably for all values of n. But we associated the number of the grid points on an interval $(0, \delta)$, for the moving grid solution, with the value of the derivative $\theta_r(r, \tau_l)$ where $r \in (0, \delta)$: the more grid points, the larger the value of the derivative.

This means that for increasing τ_l the spatial derivatives near $r = 0$ become larger. If, for a certain l, ϵ^2 is relatively small compared to the first gridpoint x_1, we have approximately for all i (for the last term in $G^{\pm}(x_i)$, see equations (71) and (73)):

$$\frac{n^2 \sin^2 u_i}{x_i^2 + \epsilon^2} \approx \frac{n^2 \sin^2 u_i}{x_i^2}. \tag{75}$$

Let u_0^L be (close to) zero. In this situation, the demand that DE cannot increase as time grows, dictates that u_0^{L+k} stays small: if u_0^{L+k} would increase with k, the term $G(x_0)$, which contributes much more to the DE than each of the terms $\frac{n^2 \sin^2 u_i}{x_i^2+\epsilon^2}$ for $i \geq 1$, would become too large, contradicting that the DE is nonincreasing.

However, the grid moves and (as a matter of fact) the number of grid points in $(0, \eta)$ becomes more numerous. This means that, if $NPTS$ is large, at a certain time τ_{L+J} we have $x_i^2 < \epsilon^2$ for $|i| < p$. For all such i, the denominator in the term

$$\frac{n^2 \sin^2 u_i}{x_i^2 + \epsilon^2}$$

and the denominator of $G(x_0)$ are approximately equal. Thus the numerator in $G(x_0)$ may grow larger without too much increase in DE. In return, growth of u_0 implies that the approximation of the derivative θ_r^2 in (71) and (73) will become smaller. The net result of the growth of u_0, for $x_i < \epsilon$ if $|i| < p$, is then a decrease in discrete energy.

Answer to Question 5.3: A possible explanation for the problem, for which values of the other parameters the "correct" numerical blow-up behaviour of $u_m^l(n, u^0)$ is seen, is the following: A sufficiently small ratio $\frac{x_1}{\epsilon}$ can cause the numerical approximation to blow up. This implies that there are wrong ways to choose these parameters, if we want to study the blow-up behaviour of θ.
□

Apart from this stands the question, whether the semi-discrete problem has numerical blow-up for a particular value of n. If we want to conclude that the semi-discrete

problem blows up we need to ensure that there is no "artificial" blow-up, like in the above argument, caused by the moving of the grid. We shall see now if the following criterion for exact blow-up works well:

Definition 5.2 *(Criterion for blow-up) We conclude that the solution θ to 10 for certain n and $\theta(r,0)$ blows up in finite time, when for the corresponding moving grid approximations $u_m^l(n, u^0, NPTS)$ (with $NPTS$ fixed and ϵ variable) it holds that numerical blow-up occurs for any small ϵ for which the code is able to compute the approximation.*

Let us consider now for various values of n, what happens when we decrease ϵ while using the fixed value of $NPTS = 101$:

$n:$	1	$\sqrt{3.5}$	2	$\sqrt{4.5}$	4
$\epsilon = 10^{-3}$	...	...	$7, 34$	...	$28, X$
$\epsilon = 10^{-4}$	$5, 17$	$8, 40$	$9, 47$	$9, 56$	X
$\epsilon = 10^{-5}$	...	...	$10, 63$	...	X
$\epsilon = 10^{-6}$	...	$10, 65$	$12, X$	...	X
$\epsilon = 10^{-7}$	$6, 23$	$17, X$	$25, X$	$36, X$	X
$\epsilon = 10^{-9}$	$6, 24$	X^*	X	X	X

For $n = 1$, the FTB-behaviour is roughly the same for varying $NPTS$, given a certain value of ϵ (the BUT only varies slightly, and the character of the FTB does not change at all). There is CBU for very large ϵ (10^{-3}). This confirms what we expected for this value of n: there is FTB twice for the particular initial value used. So for $n = 1$ the criterion 5.2 is sufficient. For $n = 4$ on the other hand, the criterion clearly shows that there is only numerical blow-up when the ϵ is small enough. This agrees with the exact blow-up behaviour as well.
However, for $n \approx 2$, according to definition 5.2, there is no FTB in the case $n = 2$ nor for the case $n = \sqrt{3.5}$. This makes definition 5.2 fail. Maybe it is possible to compute the solutions for larger blow-up times, or to use the approach suggested in section 5.7 to compute the numerical blow-up time.
□

5.7 Computation of the exact blow-up time on a large domain

Here the following troublesome fact will be discussed: suppose that we want to decide that the numerical solution u_m^l does not blow up in finite time, or in other words, that it exists for all T. We can never be sure of existence for all time as long as we have to choose finite TF. So, for example, our conclusion that the numerical blow-up behaviour (given n and an initial condition) coincides with the exact FTB-behaviour will be unfounded unless we know when for a given ϵ the exact blow-up time to (10) has been reached.

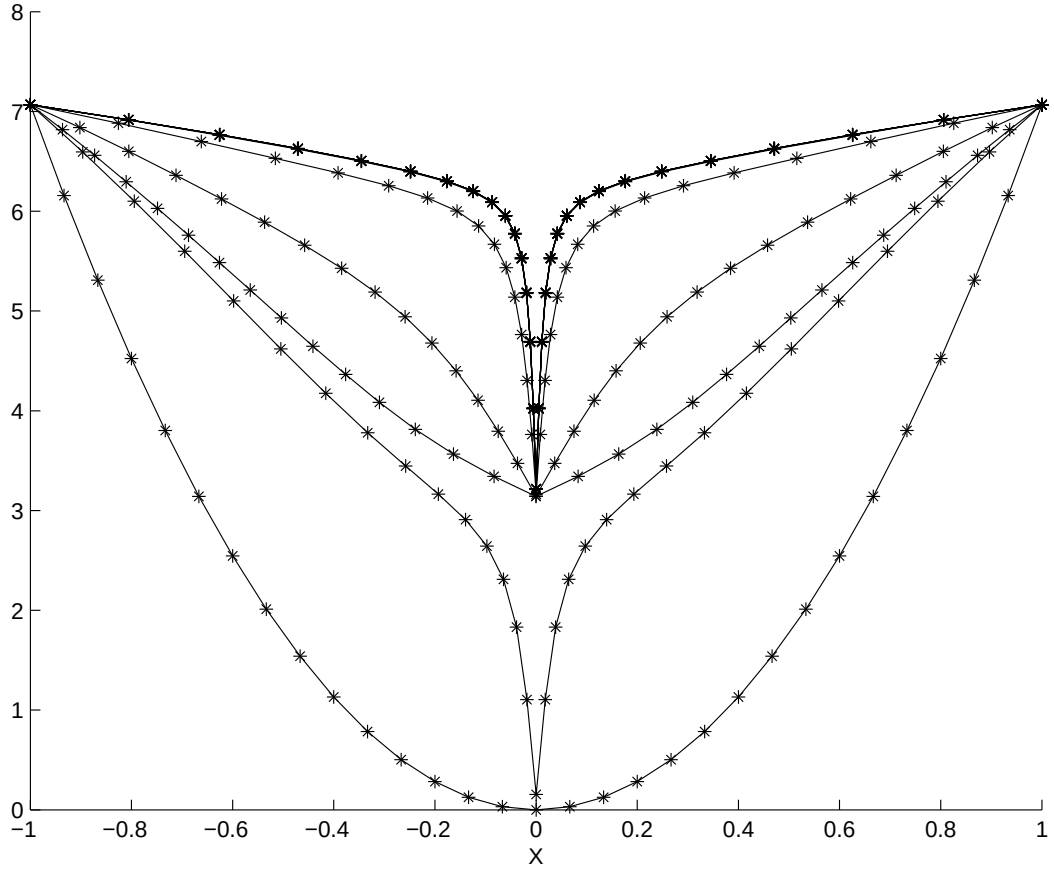

Figure 11: Moving grid approximation to (40)-(42) for $\epsilon = 10^{-7}$ and $n = 1$. Already for $NPTS = 31$ and $TF = 3$, the solution blows up numerically for quite small ϵ. In this case, the numerical blow-up is not due to the interaction between $NPTS$ and ϵ. Compare to the following figures.

In theory, there is actually a way to approximate the numerical blow-up time: one can approximate the solution to a different problem, obtained from problem (40) by a change of variables $\epsilon^2\tau = t$, $\epsilon\rho = r$. This change of variables produces the following equations, the first of which is (40) with ϵ replaced by 1, while ϵ is now in the boundary conditions:

$$\theta_t = \theta_{rr} + \frac{\theta_r}{\sqrt{r^2+1}} - n^2\frac{\sin 2\theta}{2(r^2+1)} \quad \text{for} \quad (r,t) \in \left(-\frac{1}{\epsilon}, \frac{1}{\epsilon}\right) \times \left(0, \frac{T}{\epsilon^2}\right); \tag{76}$$

$$\theta(r,0) = \theta_0(r) \quad \text{for} \quad r \in \left[-\frac{1}{\epsilon}, \frac{1}{\epsilon}\right]; \tag{77}$$

$$\theta\left(-\frac{1}{\epsilon}, t\right) = \theta\left(\frac{1}{\epsilon}, t\right) = \Theta \quad \text{for} \quad t < \frac{T}{\epsilon^2}. \tag{78}$$

When approximating this rescaled problem, one need not choose the final time of the computations very large to compute the numerical blow-up time T. Instead,

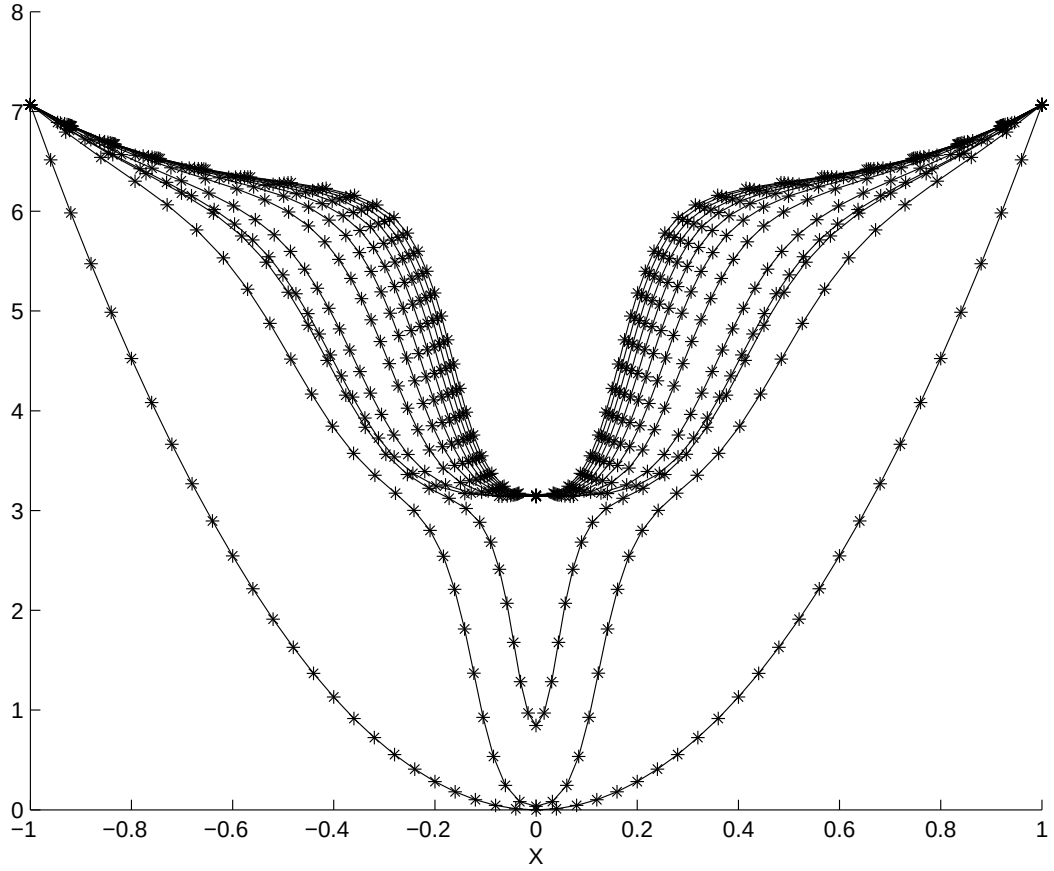

Figure 12: Moving grid approximation to (40)-(42) for $n = 4$ and $\epsilon = 10^{-2}$; $TF = 3$. $NPTS = 51$ is quite small. For such large ϵ, the approximation blows up numerically for almost all values of n and $NPTS$; we saw an explanation of this in the present section. Compare this to the next two figures, also for the case $n = 4$, but with smaller ϵ.

one takes a very large domain on which the approximation will be computed, and then one can see whether this approximation blows up in finite time. The number of gridpoints needed per time step will not be exceedingly great. So the expectation is, that the limited number of time steps needed in the approximation to this rescaled problem (76) will allow us to approximate the real BUT. Zegeling's expectation is, however, that some other computational problems will arise for his code when dealing with this problem (76).

5.8 Conclusion drawn from the numerical results

In summary, the numerical blow-up behaviour of the approximations u_m^l to (40) generated by the Zegeling scheme cannot be reconciled with the blow-up behaviour of the exact solution θ to (10) for values $n \in (2-\eta, 2+\eta)$ where this exact behaviour is known. We tried several ways to extract a criterion for numerical blow-up that matched with the exact blow-up behaviour, but we did not succeed. This means

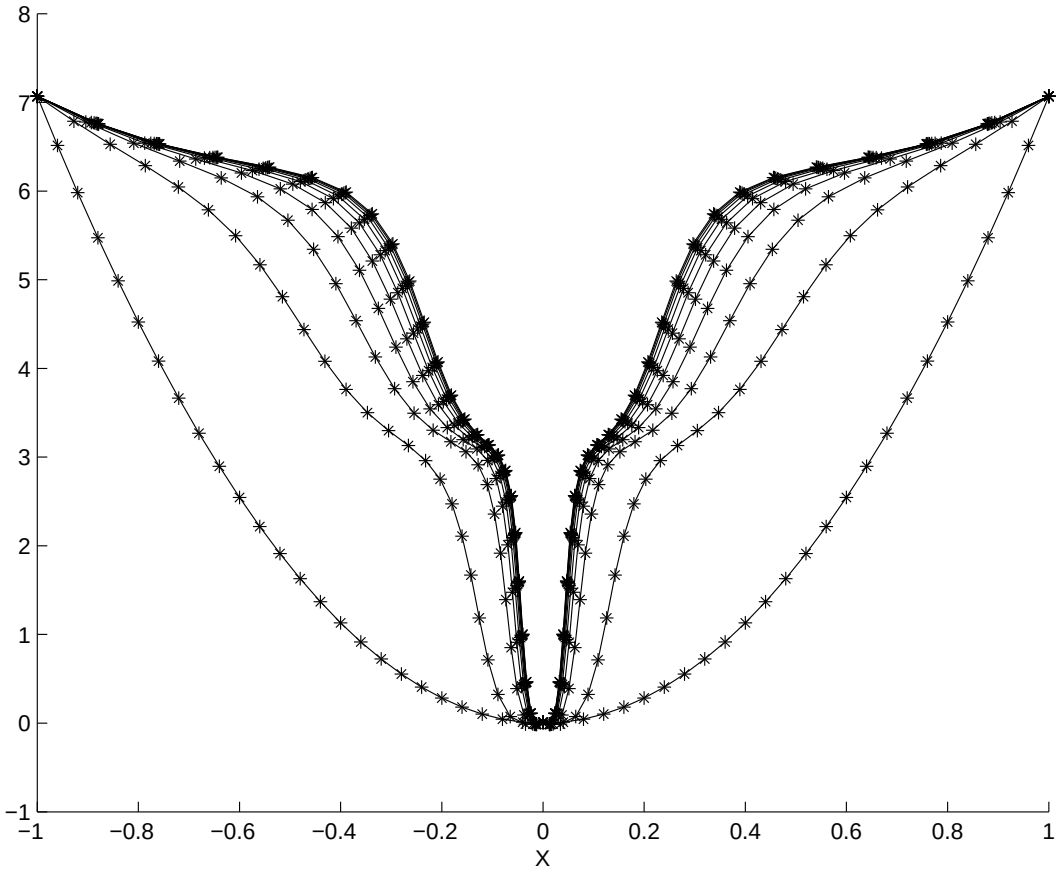

Figure 13: Moving grid approximation to (40)-(42), under the same conditions as in figure 12, except that here $\epsilon = 10^{-5}$. There is nothing like numerical blow-up anymore for this ϵ, unless we would make $NPTS$ very large.

that for the case $n = 2$ of problem (10), of which we wanted to study the blow-up behaviour by numerical methods, we cannot conclude anything yet. Maybe a suitable criterion can be found in one of the suggestions done in this chapter. We did not have the time to elaborate those suggestions.

However, we consider it to be a confirmation of the strength of the numerical method, that a marked difference between the blow-up behaviour of $\theta(r,t)$ and that of the corresponding approximations u_m^l is observed *only* near *that* value of n ($n = 2$) where the blow-up behaviour of the exact solution $\theta(r,t)$ changes its character.

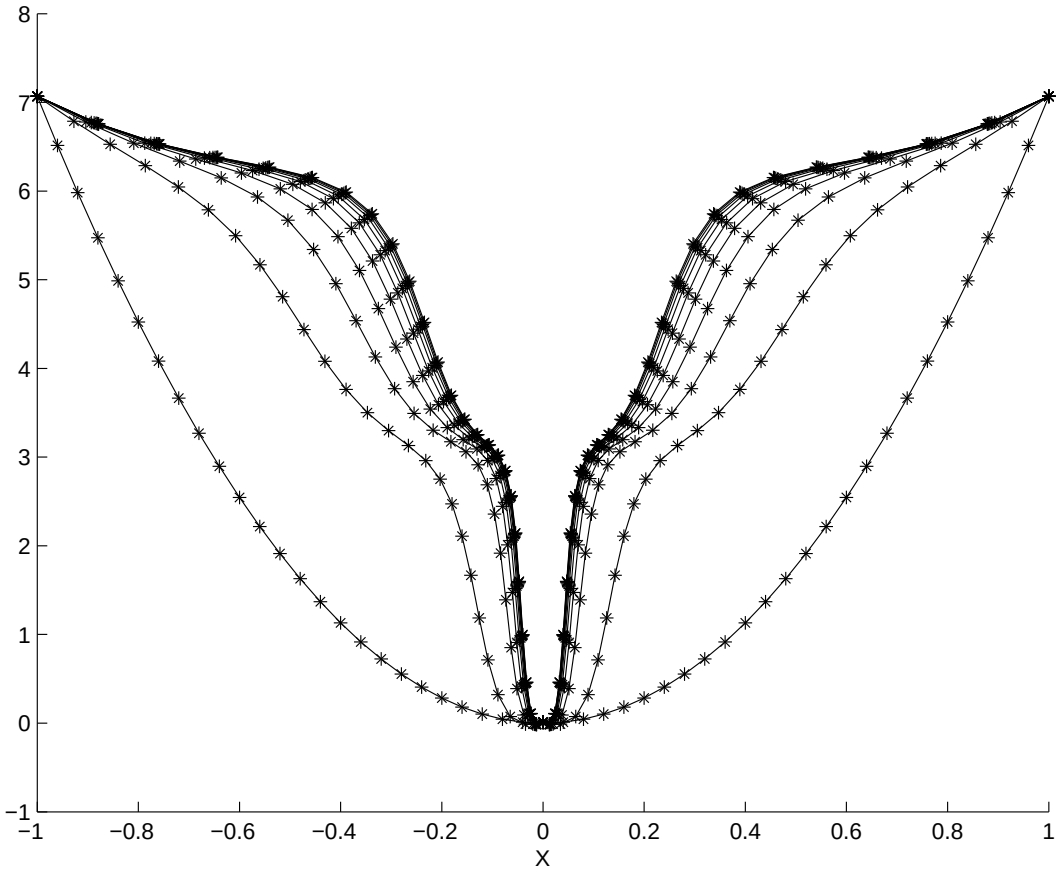

Figure 14: Moving grid approximation to (40)-(42), under the same conditions as in figure 12, except that here $\epsilon = 10^{-9}$.

6 Conclusion

6.1 Summary and conclusion

The purpose of the author's graduation research, of which this paper is part, was to find out, whether the blow-up result that was proved for the case $n = 1$ of problem (10)-(13) in [4], could be extended to the case $n = 2$ (Question 1.1). An analytical answer to this question has still not been found.

In this paper, the application of a moving grid code, developed by Zegeling, to a regularization (40)-(42) of problem (10)-(13), did not give any conclusive numerical results either.

Two semi-discrete formulations were considered in chapter 4: one corresponding to the case $\epsilon = 0$ (i.e. to equation (10)), another to the case $\epsilon \neq 0$. Although in both cases, the energy was nonincreasing in time, in the case $\epsilon = 0$ we could prove, under which conditions (on n and on the initial condition) the FTB would take place. These conditions were less strict than those in problem (10)-(13).

In contrast, when $\epsilon \neq 0$ there is no equivalent to the notion of FTB: for every value $\theta(0) = \alpha$ at the left boundary, there exists a solution to equation (51). So there is no harmonic limit solution. However, we defined numerical blow-up, and we made it acceptable by a heuristic argument, that we can expect numerical blow-up for all values of n.

We noticed the following about the numerical approximations obtained by Zegeling's code:

• All approximations u_m^l obtained using a moving grid have a discrete energy $DE(u_m^l)$ that is non-increasing in time. This does not hold for all fixed-grid approximations.

• For approximations u_m^l becoming (apparently) more precise, the numerical solution eventually (when $NPTS$ is sufficiently large, given ϵ) blows up for all n. This can be explained by assuming the discrete energy to be nonincreasing for u_m^l and then considering the influence of increasing $NPTS$ on the behaviour of the discrete energy DE. See section 5.6 on this. So we cannot draw any conclusion about the blow-up behaviour of θ just by considering more accurate approximations to (40).

• We tried if the blow-up results obtained by criterion 5.2 agreed with the known blow-up results for problem (10)-(13). This was not the case. We conclude therefore, that it is unfortunately not possible to find an answer to the Main Question 1.1 - at least not by the numerical tools that were tried in this paper.

6.2 Suggestions for further research

Some suggestions for further research have already been made in the previous sections. I will repeat and summarize them here.

• Do the numerical approximations u_m^l really satisfy an energy principle, like the exact solutions θ and θ_ϵ? A further analysis of the Zegeling code might make this clear.

• The method described in section 5.7, to deal with large blow-up times by trying to calculate them numerically, could be tried out. To do this, some adaptations in the Zegeling code are necessary.

• A criterion for the numerical blow-up of u_m^l might be found by considering $DE(u_m^{L+1}) - DE(u_m^L)$, i.e. the difference between the discrete energies directly after and before a jump has apparently occurred. After the taking into account an appropriate scaling, this difference should be at least 4π (by [7], Lemma 3.11).

• One question which has so far remained unanswered is, whether the exact solution θ_ϵ to (40)-(42) really does not blow up. One expects that it doesn't, as (40)-(42) is a regular parabolic problem with a bounded solution. If no analytical way to prove

global existence of θ_ϵ can be found, it would make much sense to study the Zegeling approximations at more detailed time-levels.

7 References

1. G. J. B. van den Berg, J. Hulshof and J. R. King, *Formal asymptotics of bubbling in the harmonic map heat flow*, SIAM J. Appl. Math. 63 (5), 2003, 1682-1717.

2. M. Bertsch, E. Vilucchi and R. van der Hout, *Blow-up phenomena for a singular parabolic problem*, Submitted for publication.

3. K-C. Chang and W-Y Ding, *A result on the global existence for heat flows of harmonic maps from D^2 into S^2*. In: Nematics, ed. J-M. Coron et al., Kluwer Acad. Publ., pp. 37-47.

4. K-C. Chang, W-Y. Ding and R. Ye, *Finite time blow-up of the heat flow of harmonic maps from surfaces*, J. Diff. Geom. 36 (1992), pp. 507-515.

5. P. H. Drazin, *Nonlinear systems*, Cambridge UP, Cambridge 1992.

6. D. Estep, *Preservation of invariant domains under discretization*, http://www.math.colostate.edu/~estep/research/talk.html (latest visit: june 2004)

7. R. van der Hout, *Alignment of nematic liquids in cylindrical flow*, Leiden 1999.

8. R. van der Hout, *Private communication*, 2003.

9. M. Struwe, *Geometric Evolution Problems*, Park City/ IAS Mathematics Series, 1996/2, pp. 259-339.

10. P. Zegeling, *Moving-grid methods for time-dependent partial differential equations*, CWI-Tract 94, Amsterdam 1993.